HOKKAIDO UNIVERSITY

Title	Revisiting discrete dark matter model: theta(13) ≠ 0 and v(R) dark matter
Author(s)	Hamada, Yuta; Kobayashi, Tatsuo; Ogasahara, Atsushi et al.
Citation	Journal of high energy physics, 2014(10), 183 https://doi.org/10.1007/JHEP10(2014)183
Issue Date	2014-10-30
Doc URL	https://hdl.handle.net/2115/57767
Rights(URL)	https://creativecommons.org/licenses/by/4.0/
Type	journal article
File Information	JHEP_2014_183.pdf

Hokkaido University Collection of Scholarly and Academic Papers : HUSCAP

Published for SISSA by Springer

Received: June 10, 2014
Revised: September 8, 2014
Accepted: September 25, 2014
Published: October 30, 2014

Revisiting discrete dark matter model: $\theta_{13} \neq 0$ and ν_R dark matter

Yuta Hamada,[a] **Tatsuo Kobayashi,**[a,b] **Atsushi Ogasahara,**[a] **Yuji Omura,**[c] **Fumihiro Takayama**[d] **and Daiki Yasuhara**[a]

[a] *Department of Physics, Kyoto University, Kyoto 606-8502, Japan*
[b] *Department of Physics, Hokkaido University, Sapporo 060-0810, Japan*
[c] *Department of Physics, Nagoya University, Nagoya 464-8602, Japan*
[d] *Yukawa Institute for Theoretical Physics, Kyoto University, Kyoto 606-8502, Japan*

E-mail: hamada@gauge.scphys.kyoto-u.ac.jp, kobayashi@particle.sci.hokudai.ac.jp, oga-atsu@scphys.kyoto-u.ac.jp, yujiomur@eken.phys.nagoya-u.ac.jp, takayama@yukawa.kyoto-u.ac.jp, yasuhara@gauge.scphys.kyoto-u.ac.jp

Abstract: We revisit the discrete dark matter model with the A_4 flavor symmetry originally introduced by M.Hirsch *et.al.* We show that radiative corrections can lead to non-zero θ_{13} and the non-zero mass for the lightest neutrino. We find an interesting relation among neutrino mixing parameters and it indicates the sizable deviation of s_{23} from the maximal angle $s_{23}^2 = 1/2$ and the degenerate mass spectrum for neutrinos. Also we study the possibilities that the right-handed neutrino is a dark matter candidate. Assuming that the thermal freeze-out explains observed dark matter abundance, TeV-scale right-handed neutrino and flavored scalar bosons are required. In such a case, the flavor symmetry plays an important role for the suppression of lepton flavor violating processes as well as for the stability of dark matter. We show that this scenario is viable within currently existing constraints from collider, low energy experiments and cosmological observations.

Keywords: Beyond Standard Model, Neutrino Physics, Discrete and Finite Symmetries

ArXiv ePrint: 1405.3592

Open Access, © The Authors.
Article funded by SCOAP[3].

doi:10.1007/JHEP10(2014)183

JHEP10(2014)183

Contents

1 Introduction **1**

2 Discrete dark matter model **2**
- 2.1 Model 3
- 2.2 Neutrino mass matrices at tree level 3
- 2.3 Dark matter candidate 4

3 Neutrino masses and mixing angles **5**

4 Right-handed neutrino dark matter **15**

5 Conclusion and discussion **20**

A A short glance at A_4 group **21**

B Scalar boson potential and the physical spectrum **22**
- B.1 Physical spectrum of scalar bosons 23

C Neutrino mass matrix and the prediction of discrete dark matter models **25**

D Radiatively induced neutrino mass structure in discrete dark matter model **26**

JHEP10(2014)183

1 Introduction

The Higgs particle, which was the last missing piece of the Standard Model (SM), has been discovered, and other precision measurements have confirmed the SM. However, still there are various mysteries on physics beyond the SM. For example, the SM has many free parameters and most of them are relevant to the flavor sector, but we have not understood what the origin of complicated flavor structure is. On the other hand, astrophysical and cosmological observations tell the existence of dark matter, but we have not understood its origin in particle physics.

The lepton sector has the specific form of mixing angles. Two of them, θ_{12} and θ_{23}, are large and the other, θ_{13}, is of $\mathcal{O}(0.1)$. In the limit, $\theta_{13} \to 0$, the Tri-bimaximal Ansatz [1–3] was a good approximation for the lepton mixing matrix, i.e. the PMNS matrix. The Tri-bimaximal matrix can be derived by using non-Abelian flavor symmetries such as A_4 and S_4 and assuming certain breaking patterns into Abelian symmetries, Z_2 and Z_3. The exact Tri-bimaximal mixing is excluded by recent experiments, which showed $\theta_{13} \neq 0$ [4–9]. However, the above approach through the use of non-Abelian discrete flavor symmetries is

still interesting to realize the lepton mixing angles with $\theta_{13} \neq 0$ as well as the quark mixing angles. (See for reviews of models with non-Abelian flavor symmetries [10–14].)

Dark matter may have heavy mass and couple with the SM particle. A certain symmetry, e.g. the R-parity in supersymmetric standard models, is useful to make dark matter stable against decays into the SM particles. Thus, the origin of dark matter may be related to the flavor structure, in particular the lepton flavor structure, and a single non-Abelian discrete symmetry may be concerned with both the realization of the lepton mixing angles and the stabilization of dark matter.

Recently, such a possibility was studied in the so-called discrete dark matter model to relate the lepton flavor structure and the origin of dark matter in refs. [15, 16].[1] The discrete dark matter model has the A_4 flavor symmetry and the A_4 symmetry is assumed to break to the Z_2 symmetry and to lead to the lepton masses and mixing angles. All of the SM particles have the Z_2 even charge, but some of right-handed neutrinos and the extra Higgs scalars coupled with only the neutrinos have the Z_2 odd charge. Thus, the lightest particle with the Z_2 odd charge must be stable. In [15, 16], the extra Higgs scalar is assumed to be a dark matter candidate. It was shown that the model leads to $\theta_{13} = 0$ and the inverted hierarchy of neutrino masses with $m_3 = 0$. One may obtain $\theta_{13} \neq 0$ by extending the model.

In this paper, we revisit the discrete dark matter model. We will show that radiative corrections can lead to $\theta_{13} = \mathcal{O}(0.1)$ and $m_3 \neq 0$ even without extending the original discrete dark matter model. Both the inverted and normal hierarchies are possible. We also study the possibilities that the right-handed neutrino is a dark matter candidate in this model.[2] In such a scenario, the typical mass scale of the model is as low as $\mathcal{O}(100 - 1000)$GeV. In general, experimental constraints such as lepton flavor violation experiments and collider bounds have already set a limit on the right-handed neutrinos and the extra Higgs scalars with such a mass scale. However, in our scenario, the breaking scale of A_4 is quite low. That leads to a characteristic phenomenology and the flavor symmetry is also helpful to evade the strong experimental constraints.

This paper is organized as follows. In section 2, we review the discrete dark matter model. In section 3, we study radiative corrections on neutrino masses. In section 4, we study the scenario that the right-handed neutrino is lighter than the extra scalar and a dark matter candidate. Several phenomenological aspects of our scenario are also studied. Section 5 is devoted to conclusion and discussion. In appendix A, we show group theoretical aspects of A_4. In appendix B, we write explicitly the scalar potential, and study the mass spectrum. In appendix C, we show in detail the neutrino mass matrix. In appendix D, we discuss radiative corrections in the neutrino masses.

2 Discrete dark matter model

In this section, we briefly review the discrete dark matter model proposed in refs. [15, 16] to give a dark matter candidate and an explanation for the flavor structure of the lepton sector simultaneously.

[1] See also [17, 19–22].

[2] See, e.g. for works on right-handed neutrino dark matter [18].

JHEP10(2014)183

	L_e	L_μ	L_τ	e_R	μ_R	τ_R	$\nu_R = (\nu_R^1, \nu_R^2, \nu_R^3)$	N_4	h	$\eta = (\eta_1, \eta_2, \eta_3)$
$\mathrm{SU(2)_L}$	**2**	**2**	**2**	**1**	**1**	**1**	**1**	**1**	**2**	**2**
A_4	**1**	$\mathbf{1'}$	$\mathbf{1''}$	**1**	$\mathbf{1''}$	$\mathbf{1'}$	**3**	**1**	**1**	**3**

Table 1. Ingredients of the model and charge assignments to them.

2.1 Model

In this model, the A_4 group, which is the symmetry group of the tetrahedron, is adopted as the lepton flavor symmetry group. A brief description of the A_4 group is given in appendix A. A_4 has four irreducible representations, that is, three singlets($\mathbf{1}, \mathbf{1'}, \mathbf{1''}$) and one triplet($\mathbf{3}$). Ingredients of the discrete dark matter model are assigned to symmetry group representations according to table 1.

$L_\alpha(\alpha = e, \mu, \tau)$ represent $\mathrm{SU(2)_L}$ doublets composed of a left-handed charged lepton and a left-handed neutrino. e_R, μ_R, τ_R are right-handed charged leptons. h is the Higgs boson. Adding to these SM particles, right-handed neutrinos $\nu_R^i(i = 1, 2, 3)$, N_4 and $\mathrm{SU(2)_L}$ doublet scalars $\eta_j(j = 1, 2, 3)$ are introduced. Each of ν_R^i and η_j are put together into A_4 triplets.

Each term in the Lagrangian must be constructed to be A_4 invariant. See appendix A to check how to multiply non trivial A_4 representations together into the trivial singlet. The terms responsible for mass matrices of charged leptons and neutrinos are given by,

$$\begin{aligned}\mathcal{L}_{\text{Yukawa}} = & \, y_e \overline{L}_e e_R h + y_\mu \overline{L}_\mu \mu_R h + y_\tau \overline{L}_\tau \tau_R h \\ & + y_\nu^e \overline{L}_e (\nu_R \tilde{\eta})_1 + y_\nu^\mu \overline{L}_\mu (\nu_R \tilde{\eta})_{1''} + y_\nu^\tau \overline{L}_\tau (\nu_R \tilde{\eta})_{1'} \\ & + Y_4 \overline{L}_e N_4 \tilde{h} + M_N \overline{\nu_R^c} \nu_R + M_4 \overline{N_4^c} N_4 + \text{h.c.}.\end{aligned} \tag{2.1}$$

The potential of scalar bosons is given in appendix B. One comment has to be addressed here. In this paper, we introduce the following A_4 soft breaking bilinear term,

$$-m_{h\eta_1}^2 \eta_1^\dagger h + \text{h.c.}, \tag{2.2}$$

which was not considered in the original paper [15, 16]. We will explain the motivation in section 4. We assume $m_\eta^2 > 0$ and $m_{h\eta_1}^2/m_\eta^2 \ll 1$ in most of discussions below. Under this assumption $m_\eta^2 > 0$ and the existence of the soft term eq. (2.2), η can acquire their non-zero vacuum expectation values(VEVs) when electroweak(EW) symmetry is violated, while light or massless scalar modes do not arise because the degrees of freedom of EW vacuum degeneracy of scalar bosons coincide with the degrees of freedom of longitudinal modes of massive electroweak gauge bosons.

2.2 Neutrino mass matrices at tree level

When scalar bosons of this model gets VEVs such that

$$\langle h^0 \rangle = v_h \neq 0, \quad \langle \eta_1^0 \rangle = v_\eta \neq 0, \quad \langle \eta_{2,3}^0 \rangle = 0, \tag{2.3}$$

JHEP10(2014)183

the neutrino Dirac mass matrix is given by

$$m_D = \begin{pmatrix} y_\nu^e v_\eta & 0 & 0 & Y_4 v_h \\ y_\nu^\mu v_\eta & 0 & 0 & 0 \\ y_\nu^\tau v_\eta & 0 & 0 & 0 \end{pmatrix} \equiv \begin{pmatrix} x_1 & 0 & 0 & y_1 \\ x_2 & 0 & 0 & 0 \\ x_3 & 0 & 0 & 0 \end{pmatrix}, \tag{2.4}$$

from (2.1). Similarly, the Majorana mass matrix of right-handed neutrinos is

$$m_R = \begin{pmatrix} M_N & 0 & 0 & 0 \\ 0 & M_N & 0 & 0 \\ 0 & 0 & M_N & 0 \\ 0 & 0 & 0 & M_4 \end{pmatrix}. \tag{2.5}$$

Then we can get the Majorana mass matrix of left-handed neutrinos from these matrices with type-I seesaw mechanism,

$$m_\nu \equiv -m_D m_R^{-1} m_D^T = \begin{pmatrix} \frac{x_1^2}{M_N} + \frac{y_1^2}{M_4} & \frac{x_1 x_2}{M_N} & \frac{x_1 x_3}{M_N} \\ \frac{x_1 x_2}{M_N} & \frac{x_2^2}{M_N} & \frac{x_2 x_3}{M_N} \\ \frac{x_1 x_3}{M_N} & \frac{x_2 x_3}{M_N} & \frac{x_3^2}{M_N} \end{pmatrix} \equiv \begin{pmatrix} Y^2 & AB & AC \\ AB & B^2 & BC \\ AC & BC & C^2 \end{pmatrix}. \tag{2.6}$$

Here, parameters which determine matrix elements are defined as

$$A, B, C = \frac{x_{1,2,3}}{\sqrt{M_N}}, \quad Y^2 = \frac{x_1^2}{M_N} + \frac{y_1^2}{M_4}. \tag{2.7}$$

We can see now why the A_4 singlet N_4 is needed. If we did not have N_4, the rank of (2.6) would be one because of (2.4), and we would get a degenerate spectrum of the left-handed neutrino masses which is excluded by experiments.

Note that eq. (2.1) leads to the diagonal mass matrix for the charged lepton sector. Thus, the PMNS matrix is determined only by the structure of the neutrino mass matrix.

At the tree level, the Majorana mass of the lightest left-handed neutrino is zero because the rank of (2.6) is two. The eigenvector corresponding to this zero eigenvalue is $(0, -C, B)^T/\sqrt{B^2 + C^2}$, which means $\sin\theta_{13} = 0$, $m_3 = 0$ when it is assumed to be the third column of the PMNS matrix. This case realizes the Inverted Hierarchy(IH) mass pattern.

2.3 Dark matter candidate

In this scenario, the A_4 flavor symmetry is broken by the vacuum alignment in eq. (2.3). The residual symmetry is Z_2 generated by

$$\begin{pmatrix} 1 & 0 & 0 \\ 0 & -1 & 0 \\ 0 & 0 & -1 \end{pmatrix}, \tag{2.8}$$

and the second and the third components of the A_4 triplets become odd under this residual Z_2 symmetry. That is, η_2, η_3, ν_R^2, and ν_R^3 belong to the Z_2 odd sector after the A_4 flavor symmetry is broken to Z_2 while all the other ingredients of this model have the Z_2 even parity. Thus, the lightest particle in the Z_2 odd sector is stable and a good candidate for dark matter.

JHEP10(2014)183

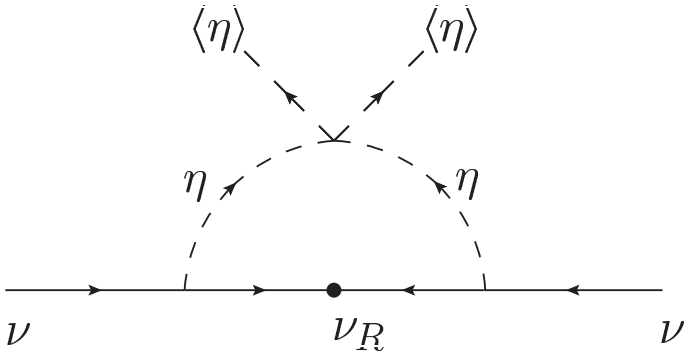

Figure 1. The one-loop diagrams contributing to A_4 breaking neutrino masses under mass insertion approximations for $m^2_{h\eta_1}/m^2_\eta$.

3 Neutrino masses and mixing angles

In this section, we investigate whether or not this model can explain both observed neutrino mass hierarchy and lepton generation mixing including non-zero θ_{13}.

The lepton flavor mixing matrix takes the form as $V_{\rm PMNS} = U_l^\dagger U_\nu$ where U_l and U_ν are unitary matrices to diagonalize the charged lepton and neutrino mass matrices. In this model, the charged lepton Yukawa couplings take diagonal form in the A_4 irreducible representation basis, we could safely take U_l to unit matrix as a good approximation and the physical lepton generation mixings arise only from the neutrino mixing matrix U_ν. In this paper, to explain non-zero θ_{13}, we consider the extension modifying only neutrino mixing matrix U_ν and we do not consider the modification of the charged lepton mixing matrix U_l because we would like to leave the Z_3 structure in charged lepton sector suppressing lepton flavor violating processes which is discussed in the next section.

As we mentioned in the previous section, the tree-level contribution to neutrino mass with N_4 discussed in the original paper [15, 16] can not achieve non-zero θ_{13}. In this paper, we consider radiative corrections to neutrino masses which were not included in [15, 16]. The one-loop diagram contributing to neutrino masses are shown e.g in figure 1, figure 2 and figure 3. In general, the four point scalar boson interactions contain complex phases and can introduce CP phases to the neutrino mass matrix. See appendix B for definitions of the quartic scalar couplings λ_a. Also we could add non-trivial singlet $N_5(\mathbf{1}')$ and $N_6(\mathbf{1}'')$. The Yukawa interactions and the mass terms are as follows,[3]

$$L^{\rm Yukawa} = Y_5 \overline{L_\mu} N_5 h + Y_6 \overline{L_\tau} N_6 h + \text{h.c.}, \tag{3.1}$$

$$L^{\rm mass} = m_{N_5} \overline{N_5^c} N_6 + \text{h.c.}. \tag{3.2}$$

Since the rephasing of $N_{5,6}$ can not remove all phases of Y_5, Y_6 and m_{N_5}, these terms can be a source of CP phase in neutrino masses. The situation for N_4 is the same as the case of $N_{5,6}$.

This model generates neutrino masses in two different ways, seesaw mechanism and radiative corrections. See for detailed studies on radiative corrections appendix D. However

[3]The modification for neutrino mass due to $N_5(\mathbf{1}')$ and $N_6(\mathbf{1}'')$ was discussed at tree level in [23].

JHEP10(2014)183

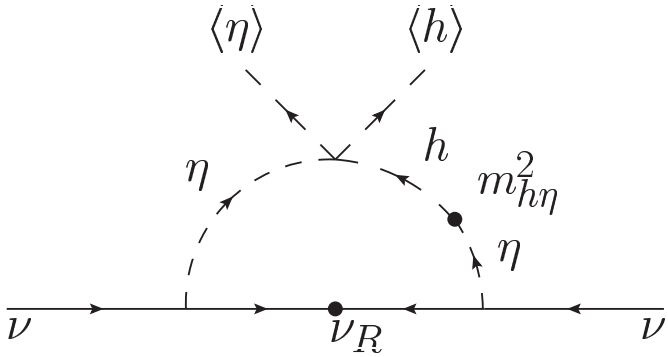

Figure 2. The one-loop diagrams contributing to A_4 breaking neutrino masses under mass insertion approximations for $m^2_{h\eta_1}/m^2_\eta$.

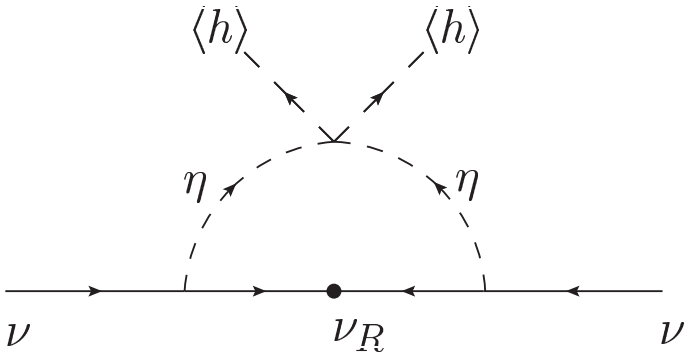

Figure 3. The one-loop diagrams contributing to A_4 symmetric neutrino masses under mass insertion approximations for $m^2_{h\eta}/m^2_\eta$.

the mass structures are classified into two types, A_4 symmetric $m_{ij}^{\rm sym}$ and A_4 violating $m_{ij}^{\rm break}$ parts in our current basis,

$$(m_\nu)_{ij} = m_{ij}^{\rm sym} + m_{ij}^{\rm break}. \tag{3.3}$$

A_4 breaking parts are introduced by picking up $\langle \eta_1^0 \rangle$ or $m^2_{h\eta_1}$. Taking the vacuum as $(\langle\eta_1\rangle, \langle\eta_2\rangle, \langle\eta_3\rangle) = (v_\eta, 0, 0)$ to leave dark matter stable, the structure of the dominant part of A_4 breaking parts takes the following form,[4]

$$m_{ij}^{\rm break} \simeq C_{\rm break} y_\nu^i y_\nu^j \frac{v_\eta^2}{m_N}, \tag{3.4}$$

with $C_{\rm break} = 1 + C_{\rm rad}^{\rm break}$, where the first term arises from the tree-level seesaw contributions by right-handed neutrinos $\nu_R^i(\mathbf{3})$ exchanges and $C_{\rm rad}^{\rm break}$ = loop factor $\times\, \lambda_{\Delta\eta=0}^{\rm break}$ from corrections. Here, we named coupling constants which give contribution to radiative corrections $\lambda_{\Delta\eta=0}^{\rm break}$. The A_4 symmetric parts can be generated through the type-I seesaw

[4]This form is a result of a condition imposed in our scalar potential. If the condition is relaxed, in general, it can be modified. See the detail in appendix B and D.

JHEP10(2014)183

mechanism by N_i $(i = 4, 5, 6)$ exchanges or radiative corrections. A_4 symmetric nature reflects into the structure of mass matrix and the non-zero elements are,

$$(m^{\rm sym})_{11} = [C^{\rm sym}_{\rm rad} y^e_\nu y^e_\nu + Y_4 Y_4 \frac{M_N}{M_{N_4}}] \frac{v_h^2}{M_N}, \tag{3.5}$$

$$(m^{\rm sym})_{23} = (m^{\rm sym})_{32} = [C^{\rm sym}_{\rm rad} y^\mu_\nu y^\tau_\nu + Y_5 Y_6 \frac{M_N}{M_{N_5}}] \frac{v_h^2}{M_N}, \tag{3.6}$$

where $C^{\rm sym}_{\rm rad}$ = loop factor $\times \lambda^{\rm sym}_{\Delta\eta=2}$, and $\lambda^{\rm sym}_{\Delta\eta=2} \sim \lambda_{11}$. $N_4(\mathbf{1})$ seesaw contributes to the 11 entry of the A_4 symmetric parts and $N_5(\mathbf{1}')$,$N_6(\mathbf{1}'')$ seesaw contributes to the 23 and 32 entries. The radiative corrections may contribute to all of 11 and 23, 32 entries. In general, $m^{\rm sym}$, $m^{\rm break}$ could be independent of each other. As one can see from (3.6), the contribution to neutrino mass matrix of $N_{5,6}$ and the A_4 symmetric parts of radiative correction enter the same mass matrix elements. Then, if scalar potential is CP invariant, we see that the same form of the neutrino mass matix is obtained in both the original discrete dark matter model including radiative corrections without $N_{5,6}$ and the model with $N_{5,6}$ neglecting radiative corrections. On the other hand, if scalar potential contains CP phases, in general, radiative corrections can introduce more freedom than the case that $N_{5,6}$ are added and only tree level contributions are considered.[5]

As we explain the detail in appendix D, for the case that the scalar potentail has the invariance for (η_2,η_3) odd permutation which may be naturally realized e.g in the case of CP invariant scalar potential, we find the following general form of neutrino mass matrix in this model,[6]

$$m_\nu = \begin{pmatrix} a^2 + X_A & ab & ac \\ ab & b^2 & bc + X_B \\ ac & bc + X_B & c^2 \end{pmatrix}. \tag{3.7}$$

We will further investigate the phenomenological consequences below. We have five complex free parameters in the neutrino mass matrix. On the other hand, taking phase redefinition of L_i $(i = e, \mu, \tau)$, for example, we can remove the phases of a, b, c and they can be taken as real numbers. Thus we have three real (a, b, c) and two complex (X_A, X_B) physical parameters. Then in such a basis, X_A and X_B can be regarded as two sources of CP phases which can not be removed by the field phase redefinition of L_i. If the all elements of (m_ν) are real, the phase redefinition arguments in this model require that $(m_\nu)_{22}/(m_\nu)_{33}$, $((m_\nu)_{11} - X_A)/(m_\nu)_{22}$ are real positive numbers.

Notice that this model predicts one relation among the elements of the neutrino mass matrices,

$$\frac{(m_\nu)^2_{12}}{(m_\nu)_{22}} = \frac{(m_\nu)^2_{13}}{(m_\nu)_{33}}. \tag{3.8}$$

[5]For example, the tree level contributions due to $N_{5,6}$ can not change the form of $m^{\rm break}$ given in eq. (3.4) but radiative corrections in the general case of CP violating scalar potential may modify the form. See the detail in appendix D.

[6]This form of the neutrino mass matrix is identical to the one considered in [24]

JHEP10(2014)183

In general, this condition is imposed on complex numbers of matrix elements. Then we have two conditions on real numbers of parameters, that is,

$$\mathrm{Re}\left(\frac{(m_\nu)_{12}^2}{(m_\nu)_{22}}-\frac{(m_\nu)_{13}^2}{(m_\nu)_{33}}\right)=\mathrm{Im}\left(\frac{(m_\nu)_{12}^2}{(m_\nu)_{22}}-\frac{(m_\nu)_{13}^2}{(m_\nu)_{33}}\right)=0. \tag{3.9}$$

Notice that for any phase basis of L_i, the above conditions for real and imaginary parts have to be satisfied.

The first question to be answered is whether this condition (3.9) is allowed or not in the current observational results. It restricts neutrino masses and mixing parameters, that is, we expect a relation among them as we will discuss it later. Taking neutrino masses as $|m_i|$ $(i=1,2,3)$ and using the conventional form of the PMNS mixing matrix,

$$U_{\mathrm{PMNS}}=VP_\nu, \tag{3.10}$$

$$V=\begin{pmatrix} c_{12}c_{13} & s_{12}c_{13} & s_{13}e^{-i\delta} \\ -s_{12}c_{23}-c_{12}s_{13}s_{23}e^{i\delta} & c_{12}c_{23}-s_{12}s_{13}s_{23}e^{i\delta} & c_{13}s_{23} \\ s_{12}s_{23}-c_{12}s_{13}c_{23}e^{i\delta} & -c_{12}s_{23}-s_{12}s_{13}c_{23}e^{i\delta} & c_{13}c_{23} \end{pmatrix}, \tag{3.11}$$

$$P_\nu=\begin{pmatrix} 1 & 0 & 0 \\ 0 & e^{i\phi_2/2} & 0 \\ 0 & 0 & e^{i\phi_3/2} \end{pmatrix}, \tag{3.12}$$

where $s_{ij}=\sin\theta_{ij}$ and $c_{ij}=\cos\theta_{ij}$, we could relate the neutrino mass matrix to observed mixing parameters, that is,

$$(m_\nu)=U_{\mathrm{PMNS}}\begin{pmatrix} |m_1| & 0 & 0 \\ 0 & |m_2| & 0 \\ 0 & 0 & |m_3| \end{pmatrix}U_{\mathrm{PMNS}}^T. \tag{3.13}$$

We list the concrete expressions for the neutrino mass matrix in appendix C. In figure 4, we show the values of the observationally preferred mass matrix elements for the case of IH mass pattern as an example by varying observable values within 3 σ of table 2. We see that there is a region where the above relation eq. (3.8) is satisfied. In following discussions, regarding m_2 and m_3 as complex numbers, $m_2=|m_2|e^{i\phi_2}$ and $m_3=|m_3|e^{i\phi_3}$, we take $P_\nu=1$ without loss of generality.

Notice that the relation eq. (3.8) has to be satisfied even in the case of previous studies [15, 16] where $\theta_{13}=0$ is taken. We easily find that $s_{23}^2=1/2$, $s_{13}=0$, $e^{-i\delta}=e^{i\phi_1}=e^{i\phi_2}=1$ satisfy the relation eq. (3.8) and it can realize the Tri-bimaximal mass pattern previously discussed in the original paper [15, 16]. In the case of non-zero θ_{13}, eq. (3.8) requires $\delta m_{12}=m_2-m_1=0$ at $s_{23}^2=1/2$ according to the discussion in appendix C. This is a trivial solution of eq. (3.8). We find the general solutions of eq. (3.8) for non zero θ_{13} by shifting δs_{23} and δm_{12} from the trivial solution and the solution sensitively constrains deviation from $s_{23}^2=1/2$, $\delta s_{23}=s_{23}-\mathrm{sgn}(s_{23})/\sqrt{2}$ as a function of other mixing parameters. This is an interesting prediction of this model. We give the exact form of δs_{23} as a function of other mixing parameters in eq. (C.18) of appendix C. Notice that $e^{i\delta}=e^{i\phi_1}=e^{i\phi_2}=1$ automatically satisfy the condition for the imaginary part of eq. (3.9).

JHEP10(2014)183

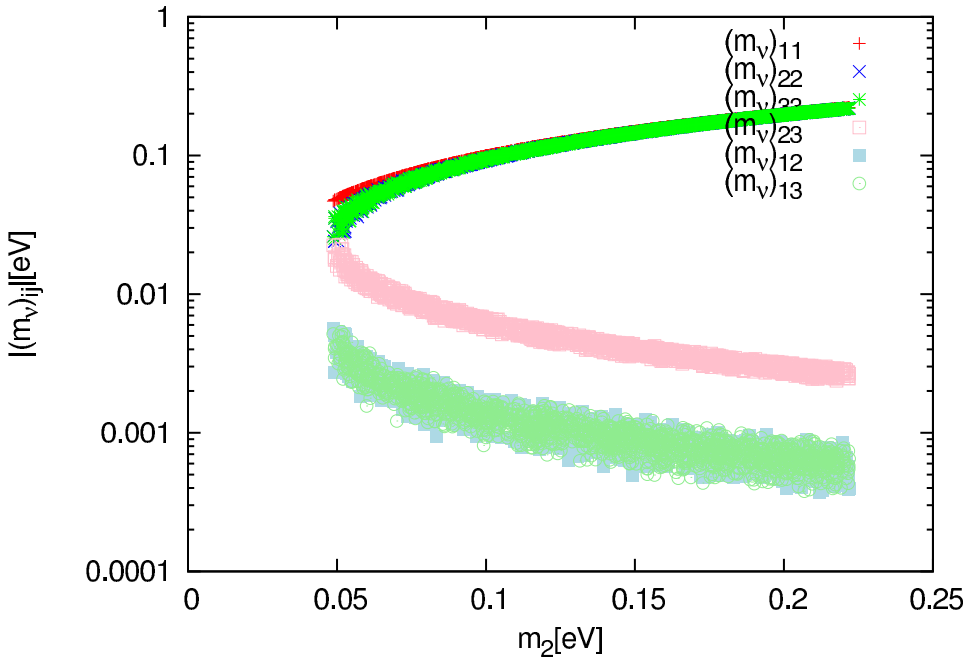

Figure 4. m_2 and observationally preferred $(m_\nu)_{ij}$ in the case of IH mass pattern with $\sum m_\nu < 0.66$eV [34].

Parameter	3σ range	best fit value
Δm^2_{21} (10^{-5}eV^2)	$6.99 - 8.18$	7.54
$\lvert\Delta m^2\rvert$ (10^{-3}eV^2)	$2.19 - 2.62(2.17 - 2.61)$	2.43(2.42)
$\sin^2\theta_{12}$	$0.259 - 0.359$	0.307
$\sin^2\theta_{23}$	$0.331 - 0.637(0.335 - 0.663)$	0.386(0.392)
$\sin^2\theta_{13}$	$0.0169 - 0.0313(0.0171 - 0.0315)$	0.0241(0.0244)

Table 2. The 3σ allowed ranges [19]. The values are in the case with $m_1 < m_2 < m_3$. The values in bracket correspond to $m_3 < m_1 < m_2$. $\Delta m^2 = m_3^2 - (m_1^2 + m_2^2)/2$ is defined.

First, we investigate the model implication to the neutrino mixing parameters under this phase condition for simplicity. Later we will relax this condition for phases.

As for the case of IH mass pattern, observations require $\delta m^2_{12}/\delta m^2_{13} \sim 3 \times 10^{-2}$ where $\delta m^2_{ij} = m_j^2 - m_i^2$, and the mass difference $\delta m_{12} = m_2 - m_1$ is always very small compared with m_1 and m_2 in this case. Near the observed values of mixing parameters, we approximately translate the relation eq. (3.8) into the following form,

$$\delta m_{12} \simeq -\gamma \times 2\sqrt{2}\frac{s_{13}}{s_{12}c_{12}}\delta s_{23}\delta m_{13}, \tag{3.14}$$

where $\gamma = m_1/(\delta m_{13} + 2m_1)$ and $\delta m_{13} = m_3 - m_1$. It is easy to see that this relation can be satisfied within the current observational results at 3σ level[7] and we find a tight correlation between the smallness of δm_{12} and δs_{23}. By using the best fit values for masses

[7]We used a global fit result [25]. There are the other similar studies [26, 27]. These are consistent each others at 3σ level, but there is a difference in the allowed regions within 2σ level due to the different

JHEP10(2014)183

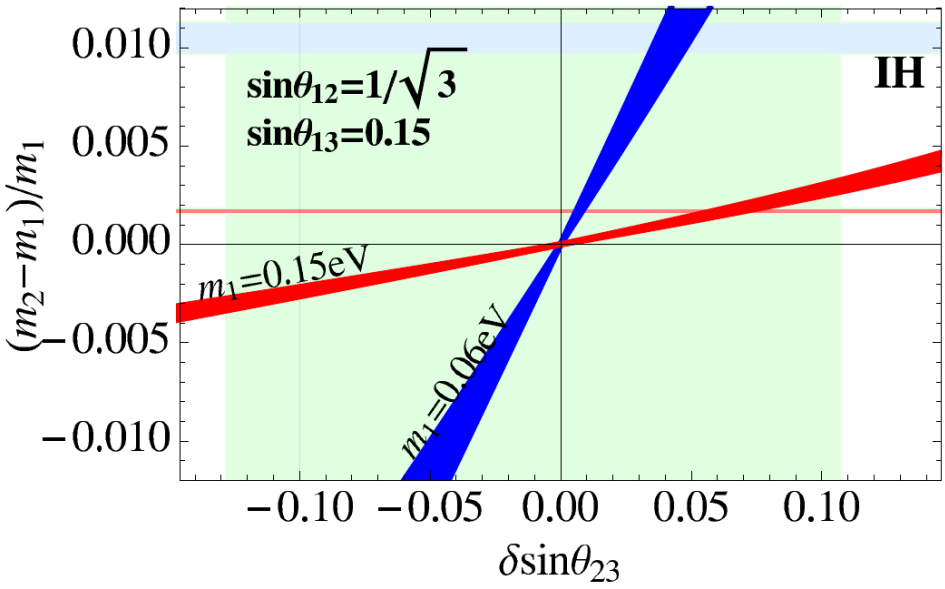

Figure 5. δs_{23} and $\delta m_{12}/m_1$ in the IH case with $s_{23} > 0$, $s_{12} = 1/\sqrt{3}$ and $s_{13} = 0.15$. The red (blue) line is the prediction of our A_4 model with $m_1 = 0.15(0.06)$eV, within 3σ of $|\Delta m^2|$. The light green region for the 3σ allowed range of $\sin^2\theta_{23}$, and the light pink (blue) band for the one of Δm^2_{12} with $m_1 = 0.15(0.06)$eV respectively.

and mixing parameters shown in table 2 and leaving s_{23} as a free parameter, we could see that the maximal angle $s^2_{23} = 1/2$ is excluded for non zero θ_{13} but s^2_{23} still has to be close to 1/2 and we find $\delta s_{23} \sim +0.015$ for the case of $\delta m_{13} \sim m_1$ ($m_1 \sim 0.05$eV) and $\delta s_{23} \sim +0.06$ for the case of $m_1 > \delta m_{13}$ ($m_1 > 0.1$eV). By using the exact form of δs_{23} eq. (C.18) and varying the values of s_{12}, s_{13} within current 3σ errors of table 2, we can still see the qualitatively same results as shown in figure 5.

In a similar way, we investigate the case of normal hierarchy (NH) mass pattern. In the case of $m_1 > \delta m_{13}$ which realizes degenerate spectrum for three neutrinos, the mass hierarchy $\delta m_{12} \sim 3 \times 10^{-2} \delta m_{13}$ is required by experimental results. In this case, we find the same approximated relation given in the previous IH case, eq. (3.14). The difference between the NH case and the IH cases is only the sign of δm_{13}. The observed mass hierarchy and mixing angles require $\delta s_{23} \sim O(0.1)$ and we find that $\delta s_{23} \sim -0.06$ is preferred if we assume $m_1 \gg \delta m_{13}$. Notice that the sign of δs_{23} is opposite to the IH case and the negative sign is preferred by the global fit of experimental data [25]. Increasing the value of $\delta m_{13}/m_1$ up to ~ 1 , δs_{23} increases up to ~ 0.15 and it reaches outside of the 3σ allowed region of $\delta s_{23} > 0.12$. For $\delta m_{13} > m_1$, the approximation of eq. (3.14) is not always valid and we numerically checked that for $m_1 < 0.04$eV, δs_{23} reaches outside of allowed region of experimental data in the case. This is again numerically confirmed in figure 6.

To see the above statements, we show the scatter plots for both IH (figure 7) and NH (figure 8) cases where all mixing parameters except for s_{23} are varied within the 3σ range

treatment of observational data. There are recent developments measuring s_{23} precisely. For examples, if we use T2K [28] seriously, then $s^2_{23} = 1/2$ is still allowed enough. On the other hand, MINOS results [29] seems a little bit disfavoring $s^3_{23} = 1/2$.

JHEP10(2014)183

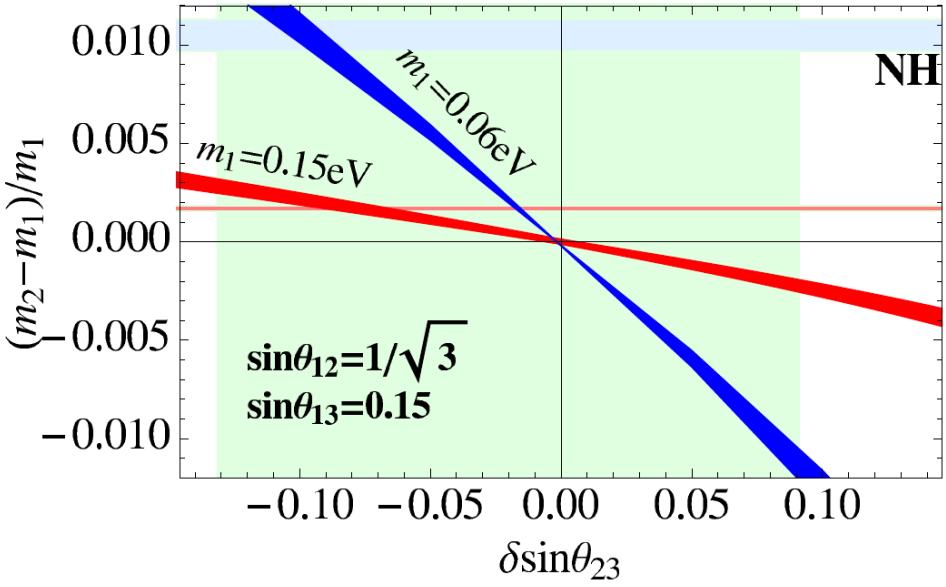

Figure 6. δs_{23} and $\delta m_{12}/m_1$ in the NH case with $s_{23} > 0$, $s_{12} = 1/\sqrt{3}$ and $s_{13} = 0.15$. The red (blue) line is the prediction of our A_4 model with $m_1 = 0.15(0.06)$eV, within 3σ of $|\Delta m^2|$. The light green region for the 3σ allowed range of $\sin^2\theta_{23}$, and the light pink (blue) band for the Δm^2_{12} with $m_1 = 0.15(0.06)$eV respectively.

given in table 2. For both NH and IH, non zero θ_{13} excludes the possibility of $s^2_{23} = 1/2$, and the tight correlation of the smallness of δs_{23} and δm_{12} exists. This is a robust prediction of this model. The deviation from s_{23} obtain $0.01 < |\delta s_{23}| \lesssim 0.1$ for $|\delta m_{13}| \lesssim m_1$ and increasing $\delta m_{13}/m_1$, $|\delta s_{23}|$ increases and it reaches outside of experimentally allowed range when we take $m_1 \lesssim 0.03$eV .

Until now, we considered only the case that all Majorana phases and Dirac CP phase are trivial. Taking account for the effect of Majorana phases, for example, we can change the sign of m_2 and m_3, that is, taking $\phi_1 = 0, \pi$, $\phi_2 = 0, \pi$. In this case, the approximated form eq. (3.14) is not always valid, especially for $m_2 < 0$ cases. We use eq. (C.18) to determine s_{23} satisfying condition eq. (3.8) without any approximation, and estimate δs_{23} for several combinations of the sign of m_2, m_3. We show the results in figure 9. Also, in appendix C, we notice $\delta s_{23} \propto s_{12}s_{13}$. As the result, for the change of the sign of s_{12}, s_{13}, the flip of the sign of $s_{12}s_{13}$ causes the flip of the sign for δs_{23}. If we include Dirac CP phase δ for real m_1, m_2, m_3, $\sin\delta = 0$ is one of the solution, which obtain $e^{-i\delta} = \pm 1$. The effect is identical to the effect of the sign flip of s_{13}.

From figure 10, we find that the solutions for IH and NH cases are allowed by the current neutrinoless double beta decay experiments [31–33], and we may expect the observation or the exclusion of the large parts in future. In this degenerate mass spectrum, as we see in figure 11, $m_1 \gtrsim 0.07\text{eV(NH)}, 0.08\text{eV(IH)}$ faces a milder tension with the results of recent Planck CMB observation by seriously taking the BAO data, but it may be still allowed in general if we do not combine the Planck data with the BAO data [34]. Also variations of $N_{\nu\text{eff}}$ from the SM value may obtain milder constraints on $\sum m_\nu$ [34]. How-

JHEP10(2014)183

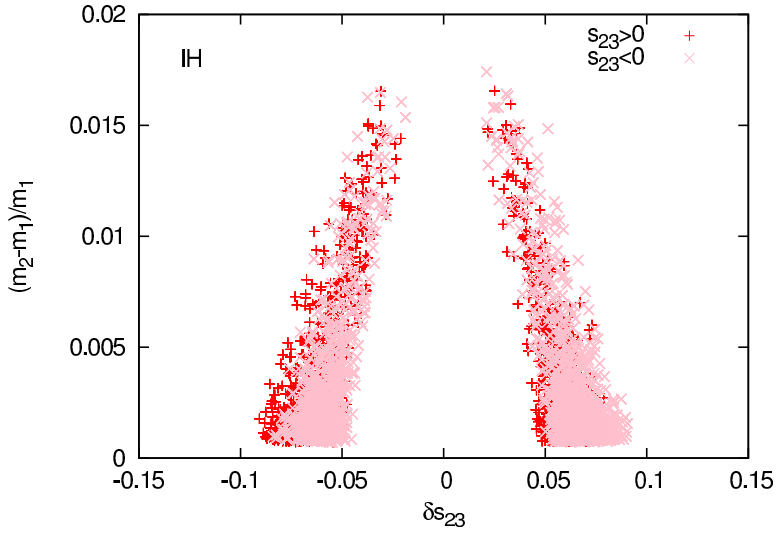

Figure 7. The scatter plot showing the A_4-model-inspired allowed region for δm_{12} and δs_{23} in IH mass pattern. The mixing parameters s_{12}, s_{13} are taken within the 3σ allowed range in table 2. Increasing m_1 obtains decreasing observationally preferred $\delta m_{12}/m_1$.

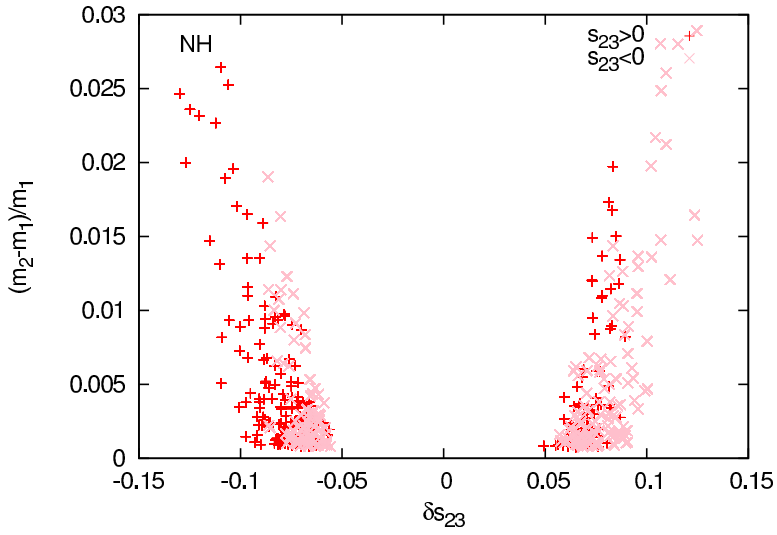

Figure 8. The scatter plot showing the A_4-model-inspired allowed region for δm_{12} and δs_{23} in NH mass pattern. The mixing parameters s_{12}, s_{13} are taken within the 3σ allowed range. Decreasing m_1 indicates increasing observationally preferred $\delta m_{12}/m_1$.

ever, too large $m_1 > 1$eV has been already excluded by both the neutrinoless double beta decay experiments and the cosmological observations.

Once we specify the observationally allowed mixing parameters and mass hierarchy where the above one relation is simultaneously satisfied, we could determine the all values of neutrino mass model parameters in turn, that is, model parameters of eq. (3.7) are

JHEP10(2014)183

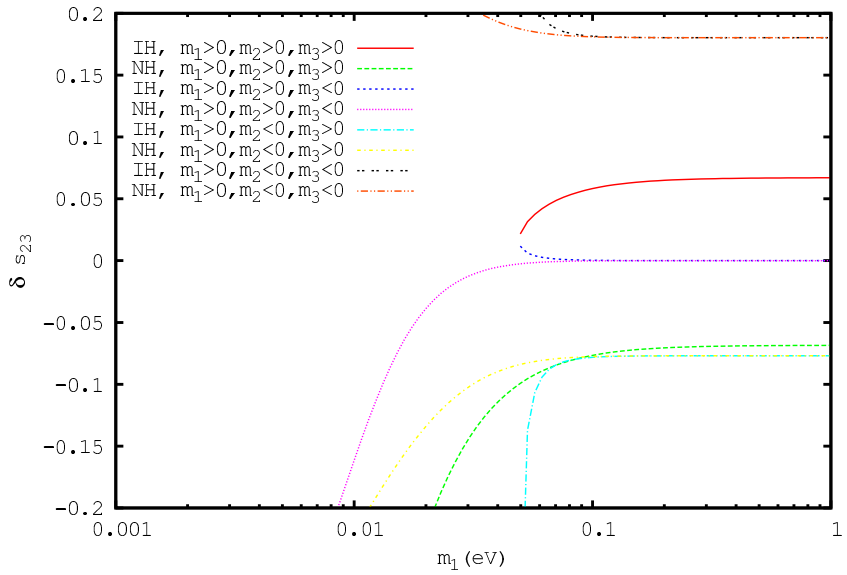

Figure 9. We show the plot for δs_{23} vs m_1 for the various cases when we take different Majorana phase (0 or π) for m_2 and m_3. We assumed $s_{12} > 0$ and $s_{13} > 0$ and we fixed δm^2_{12}, δm^2_{13}, s^2_{12} and s^2_{13} to the best fit values in table 2. When we flip the sign of s_{13}, s_{12}, the sign of δs_{23} flips as sign of $s_{12}s_{13}$. As for the change of sign of s_{23}, the sign of δs_{23} is unchanged.

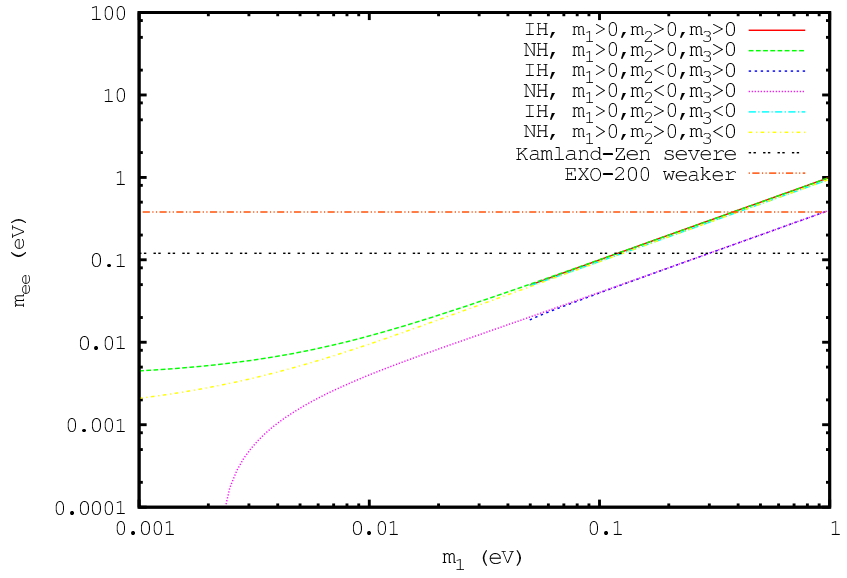

Figure 10. We show the constraints on m_1 imposed by KamLAND-Zen and EXO-200 results for neutrinoless double beta decay.

JHEP10(2014)183

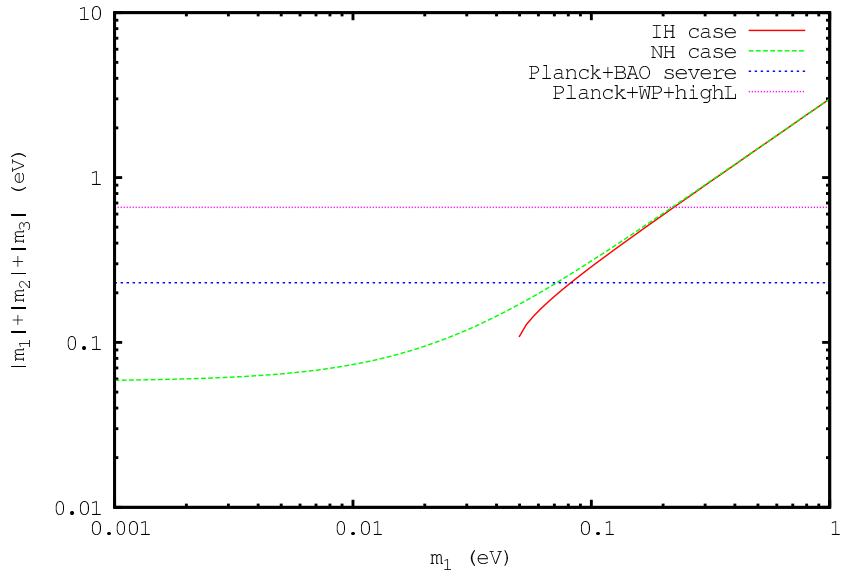

Figure 11. We show the constraints on m_1 imposed by cosmological observation of Planck satellite. The lower horizontal line corresponds to the combined constraint with BAO and the upper horizontal line corresponds to the combined constraint with WMAP and high red shift survey.

written by

$$a^2 = \frac{(m_\nu)_{12}^2}{(m_\nu)_{22}} = \frac{(m_\nu)_{13}^2}{(m_\nu)_{33}}, \tag{3.15}$$

$$b^2 = (m_\nu)_{22}, \tag{3.16}$$

$$c^2 = (m_\nu)_{33}, \tag{3.17}$$

$$X_A = (m_\nu)_{11} - a^2 = (m_\nu)_{11} - \frac{(m_\nu)_{12}^2}{(m_\nu)_{22}}, \tag{3.18}$$

$$X_B = (m_\nu)_{23} - bc. \tag{3.19}$$

In figure 12, we show the preferred values for the above model parameter a which may be an important coupling for ν_R searches in electron-positron colliders when η bosons are heavy. We find that for m_1, m_2, $m_3 > 0$ cases, the coupling takes very small values and it makes the search difficult in the case that only the production of a ν_R pair is kinematically allowed.

If we do not include N_4, N_5, N_6, under the assumption of CP invariance in our scalar potential, since radiative corrections obtain universal contributions to X_A, X_B except for the neutrino Yukawa coupling dependencies, non-zero A_4 symmetric mass matrix elements become

$$(m^{\rm sym})_{11} = C_{\rm rad} y_\nu^e y_\nu^e, \tag{3.20}$$

$$(m^{\rm sym})_{23} = (m^{\rm sym})_{32} = C_{\rm rad} y_\nu^\mu y_\nu^\tau. \tag{3.21}$$

As a result, another relation has to be imposed,

$$\frac{(m_\nu)_{12}}{(m_\nu)_{22}} \times \frac{(m_\nu)_{13}}{(m_\nu)_{33}} = \frac{(m_\nu)_{11}}{(m_\nu)_{23}}. \tag{3.22}$$

JHEP10(2014)183

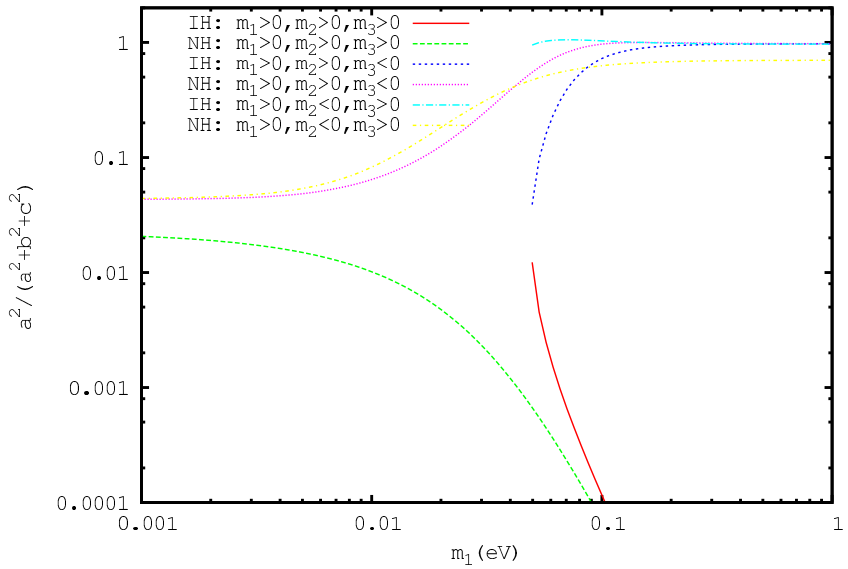

Figure 12. We show the plot for the value of $a^2/(a^2+b^2+c^2)$ which correspond to $(y_\nu^e)^2$ when we take $\sum_{i=e,\mu\tau}(y_\nu^i)^2 = 1$. The values of a, b, c are given in eq. (3.15)-(3.19) satisfying condition eq. (3.8). We assumed $s_{12} > 0$ and $s_{13} > 0$ and we fixed δm^2_{12}, δm^2_{13}, s^2_{12} and s^2_{13} to the best fit values in table 2.

We find that when we impose the first condition eq. (3.8), the case where this second condition (3.22) is simultaneously satisfied within the 3σ range of [26, 27] does not exist in the case of real m_1, m_2 and m_3. In such a case, N_4 (and/or N_5, N_6) is necessarily required to explain the observed neutrino mass structure.

On the other hand, throughout this paper, we have not investigated general cases for CP phases. The limited analysis may not obtain the complete information of the prediction of this model. We will present further analysis for general cases of CP phases elsewhere in future.

4 Right-handed neutrino dark matter

In this model, as we have seen it in section 2, the A_4 breaking due to the vacuum alignment $(\langle\eta_1\rangle, \langle\eta_2\rangle, \langle\eta_3\rangle) = (v_\eta, 0, 0)$ leaves a Z_2 generator of A_4 corresponding to a parity operator unbroken and make the lightest parity odd particle stable which can become a viable dark matter candidate. In this sense, both of η_i and ν_R^i (i=2,3) can be dark matter candidates. In past studies along with A_4 discrete dark matter models [15, 16], only the case that η_i are dark matters has been considered. In this paper, we investigate another case where right-handed neutrino ν_R^i becomes dark matter and pursue the possibility where the thermal freeze-out in early universe obtains the desired relic density required in the current cosmological observations [34].

To make ν_R^i stable, the masses (m_N) have to be lower than η_i masses, and assuming that ν_R^i obtain the desired relic density through the thermal freeze-out phenomena, Yukawa couplings (y_ν^i) should be sizable and TeV scale η and ν_R are required. In such a situation,

JHEP10(2014)183

to realize the observed small neutrino masses, v_η at sub MeV range is required as we will discuss the detail below.

In the case of spontaneous A_4 breaking taken in the past studies [15, 16], η masses are related to the EW symmetry breaking scale v_h or v_η. The smallness of v_η makes some of scalar particles light and the other modes obtain EW-scale masses, which may make the viable model building difficult for ν_R^i dark matter scenario. Hence we introduce the following soft A_4 breaking term to make all modes of η heavy,

$$L^{\rm soft} = -m_{h\eta_1}^2 \eta_1^\dagger h + \text{h.c.}. \tag{4.1}$$

This term develops the desired breaking pattern in the η VEVs and approximately we find $v_\eta \simeq m_{h\eta_1}^2/m_\eta^2 \times v_h \sim 0.1$MeV if $m_{h\eta_1}^2/m_\eta^2 \sim 10^{-6}$. Such smallness of the soft term coupling may be realized if the mediation scale of A_4 breaking is significantly higher than the A_4 breaking scale in hidden sector or if the couplings are non-perturbatively generated. We leave the discussion for future work and just assume the smallness in our following studies.[8] By the inclusion of this soft term, the physical spectrum of η particles can be independent from the EW symmetry breaking scale v_h and A_4 breaking scale v_η. We show the physical spectrum of scalar sector in appendix B.

Explaining the observed smallness of neutrino masses, we find

$$m_\nu \sim 0.1\text{eV} \left(\frac{y_\nu}{0.3}\right)^2 \left(\frac{v_\eta}{0.1\text{MeV}}\right)^2 \left(\frac{1\text{TeV}}{m_N}\right). \tag{4.2}$$

Also the observed small neutrino masses require small couplings for η number violating couplings,[9] $\lambda_{11} \sim O(10^{-8})$ and heavy N_4 (and/or N_5, N_6), $M_4 \sim 10^{13}$GeV ($m_{N_5} \sim 10^{13}$GeV) when the Yukawa couplings Y_i $(i = 4, 5, 6)$ are of $O(1)$.[10]

Next we evaluate the relic density of ν_R dark matter. In this model, the masses of ν_R^i $(i = 1, 2, 3)$ are degenerate at the tree level and the mass splitting arises through loop corrections by picking up A_4 breaking v_η. We have to understand the roles of heavier ν_R state in thermal history. The leading contributions for the mass splitting are introduced through following dimension five operators,

$$L_{m_\eta} = \frac{M_N}{\Lambda^2}[\eta^\dagger[\eta[\overline{\nu_R^c}\nu_R]_{\mathbf{3}}]_{\mathbf{3}}]_{\mathbf{1}}, \tag{4.3}$$

$$L_{m_{h\eta}} = \frac{M_N}{\Lambda^2}\frac{m_{h\eta_1}^2}{m_\eta^2}[\eta^\dagger h[\overline{\nu_R^c}\nu_R]_{\mathbf{3}}]_{\mathbf{1}}, \tag{4.4}$$

[8] In general, such a mechanism which introduces the A_4 violating soft term may generate other small A_4 breaking terms, for an example, yukawa coulings like flavor violating $\bar{L}_e \tau_R \eta_1$ and flavor conserving $\bar{L}_e e_R \eta_1$. On the other hand, for the inclusion of such possible A_4 breaking terms, if the desired A_4 breaking pattern is preserved, such couplings are also suppressed $\lesssim 10^{-6}$ as well as the soft term, and the conclusions in our paper are basically unchanged. If we consider the radiative corrections, such η_1 number violating dimensionless terms can generate soft term $m_{h\eta_1}^2 \eta_1^\dagger h$ through quantum corrections. When the A_4 breaking scale is higher than weak scale and $m_{h\eta_1} \sim O(1\text{GeV})$, the A_4 violating dimensionless couplings must be $\ll O(10^{-6})$. This may mean that our bilinear term may be induced by radiative corrections and only the term has phenomenological significances for physics we discussed in this paper.

[9] This 4-point interaction violates η number by $\Delta\eta = 2$ and can be independent from the other terms with $\Delta\eta = 0$, 1 in the origin.

[10] Very small Yukawa and TeV-scale m_{N_i} $(i = 4, 5, 6)$ might be still viable, in this paper, we do not discuss the possibility further more.

JHEP10(2014)183

where Λ is a cut-off scale. It is expected $\Lambda \gg m_\eta$ and the mass splitting may be smaller than neutrino mass m_ν. These terms are proportional to M_N because they would be related to the mechanism to realize TeV scale Majorana mass M_N. As for parity-even ν_R^1, since the decay into ν_R^i and two leptons is suppressed due to the very small mass splitting, it can dominantly decay to SM particles, $\nu_R^1 \to h + \nu$ through a mixing between the standard model Higgs and η_1 bosons,

$$\tau_{\rm even}^{-1} \sim \frac{y_\nu^2}{32\pi}\left(\frac{m_{h\eta_1}^2}{m_\eta^2}\right)^2 \frac{m_N^2 - m_h^2}{m_N} \sim [10^{-14}{\rm sec}]^{-1}\left(\frac{y_\nu}{1.0}\right)^2\left(\frac{m_{h\eta_1}^2/m_\eta^2}{10^{-6}}\right)^2\left(\frac{m_N}{500{\rm GeV}}\right), \quad (4.5)$$

where $y_\nu^2 = \sum_{i=e,\mu,\tau}(y_\nu^i)^2$ is defined. This means that for $y_\nu \sim O(1)$, the parity-even ν_R^1 can be short-lived enough and it may not disturb the thermal relic estimation of ν_R^i by the late decays. In the case for parity-odd ν_Rs, due to the very tiny mass splitting between heavier and lighter states, the decay of the heavier state to the lighter state may be introduced through the transition magnetic moments of ν_R^i,

$$L_\eta = \frac{c_\eta}{\Lambda^3}[\eta^\dagger[\eta[\overline{\nu_R^c}\sigma^{\mu\nu}\nu_R]_{\mathbf{3}}]_{\mathbf{3}}]_{\mathbf{1}}F_{\mu\nu}, \quad (4.6)$$

$$L_{\eta h} = \frac{c_{\eta h}}{\Lambda^3}\frac{m_{h\eta_1}^2}{m_\eta^2}[\eta^\dagger h[\overline{\nu_R^c}\sigma^{\mu\nu}\nu_R]_{\mathbf{3}}]_{\mathbf{1}}F_{\mu\nu}. \quad (4.7)$$

Once A_4 symmetry is broken by v_η, the above interaction generates off diagonal elements and contributes to the decay of heavier state ν_R^h to lighter state ν_R^l $\nu_R^h \to \nu_R^l + \gamma$.[11] The gamma line has very small width and it is very soft $E_\gamma < m_\nu$. We find that the lifetime of the heavier state is longer than the age of the universe,

$$\tau_{\rm odd}^{-1} \sim \frac{c_\eta^2}{64\pi}\frac{v_\eta^4}{\Lambda^6}(\delta m_N)^3 < \frac{\alpha}{64\pi}\frac{m_\nu^5}{m_\eta^4} < 10^{-23}\tau_U^{-1}, \quad (4.8)$$

where δm_N is the mass difference between ν_R^2 and ν_R^3 and $\tau_U \sim 13.8$Gyears. It may be difficult to detect this line spectrum in CMB at present [35]. This model realizes multi-state dark matter ν_R^2 and ν_R^3 at present time.

The main annihilation process of ν_R^is happens through the process shown in figure 13 and the P-wave dominates for the thermal relic estimation. The cross section is roughly,

$$\sigma_{\rm ann} v_{\rm rel} \sim 1{\rm pb} \times \left(\frac{v_{\rm rel}^2}{0.1}\right)\left(\frac{y_\nu^2}{0.3}\right)^2\left(\frac{m_N}{1{\rm TeV}}\right)^2\left(\frac{1{\rm TeV}}{m_\eta}\right)^4, \quad (4.9)$$

where $v_{\rm rel}$ is the relative velocity of incident two dark matter particles. In the thermal relic estimation, we deal with the two states of ν_R^i as stable. In figure 14, we show the preferred values of η, ν_R masses and neutrino Yukawa coupling to obtain full amount of observed dark matter relic density [34]. Now we understand that in this model, WIMP type dark matter scenario can be achieved by TeV-scale ν_R and η, sub MeV v_η and $O(1)$ neutrino Yukawa couplings. Here we did not include co-annihilation processes like $\eta_i + \nu_R^i \to l^* \to l +$ a gauge boson(W, Z, γ). Such processes are relevant only if the masses of ν_R^i highly degenerate with those of η_i.

JHEP10(2014)183

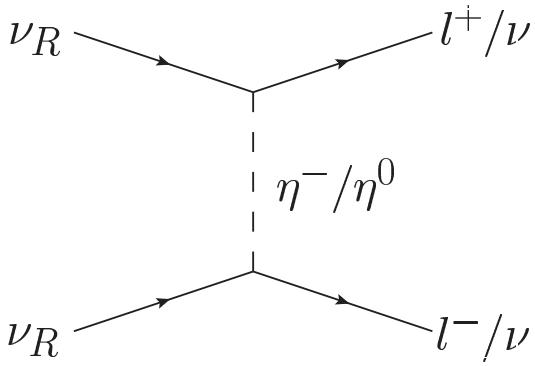

Figure 13. The main annihilation process for ν_R dark matter during the thermal freeze out.

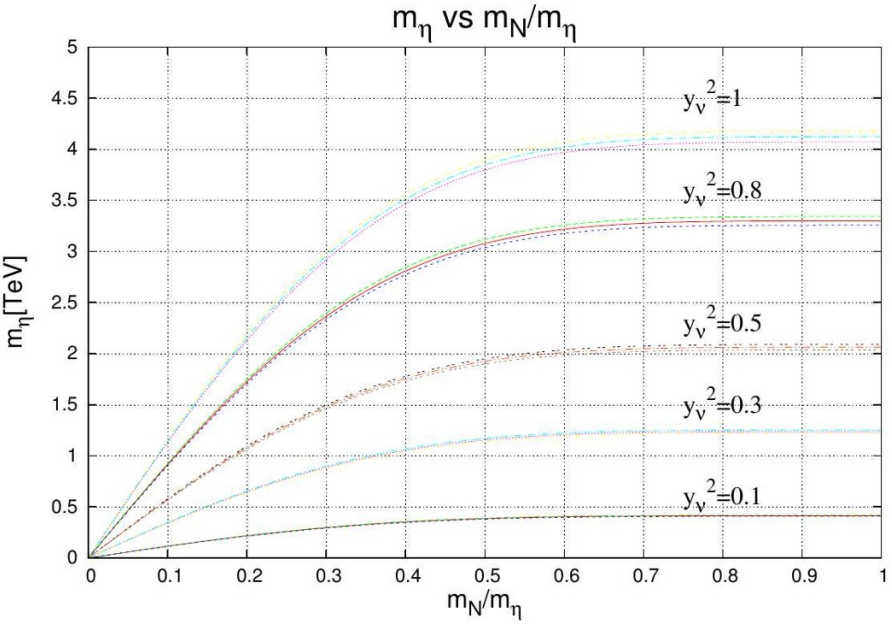

Figure 14. The values of m_η and m_N that give the observed relic abundance of dark matter in the case of ν_R dark matter scenario.

The collider signals for parity-odd η bosons are similar to R-parity conserving minimal supersymmetric standard model(MSSM) with bino dark matter except for the production rate. This model has only the pure electroweak productions at the LHC. The direct EW production of left-handed sleptons producing multi-lepton final state receives the LHC constraints as $m \gtrsim 300$GeV at ATLAS [36] and $m \gtrsim 300$GeV at CMS [37] depending on the mass splitting of the lightest supersymmetric particle and slepton. These constraints include the Drell-Yan production.[12] We find enough allowed parameter spaces to realize thermal freeze out scenario to obtain desired relic density. As for parity-even η_1, since v_η is

[11] $L = \frac{c^R_{ij}}{\Lambda}\overline{\nu^c_R}^i \sigma^{\mu\nu}\nu^j_R F_{\mu\nu}$ vanishes because of the Majonara nature of ν_R and A_4 nature.

[12] Gauge boson fusion process also exists. The s-channel process is highly suppressed due to the smallness of v_η. Thus, t-channel process is the dominant process, but it would be small compared with Drell-Yan processes.

JHEP10(2014)183

very small and the di-boson decay mode is suppressed, the primary decay is similar to the case of parity-odd η bosons though, the decay products contain parity-even ν_R^1 decaying to a Higgs and a light neutrino. ν_R^1 may be long-lived, which might leave the displaced track in collider detectors.

Here we consider the possibility for dark matter indirect detections. Again the situation is similar to the case of bino dark matter in MSSM, but it differs in the coupling of DM-lepton-η which is not fixed by hypercharge gauge coupling. Since the dominant $2 \to 2$ annihilation process is velocity suppressed or chirality suppressed, radiative processes like $\nu_R + \nu_R \to \gamma + l\bar{l}$ may become important [38–41] and the gamma ray signals have the characteristic properties on the spectrum [38–40]. Other indirect detections of these types of dark matter through charged cosmic rays and neutrinos have been intensively studied in past papers [42–45].

In this model, when v_η goes to zero, η and ν_R couple with only left-handed leptons which do not contribute to the lepton transition magnetic moments at one-loop level. It is expected that a small contribution arises at two loop level from figure 15. The situation is similar in the loop contributions through N_i $(i = 4, 5, 6)$ which also do not directly couple with right-handed charged leptons.[13] Such loop contributions may be described by the following dimension six operator,

$$L = \frac{c_{ij}}{\Lambda^2} \overline{L}_i h \sigma^{\mu\nu} (e_R)_j F_{\mu\nu}, \tag{4.10}$$

where c_{ij} are $O(1)$ numerical coefficients, Λ is a cut off scale of effective operators and it is expected to be higher than η mass scale. We might expect the lepton flavor violating(LFV) contributions like $\mu \to e\gamma$, $\tau \to e\gamma$ due to the dimension six operator, however, when we ignore the v_η/v_h, this term can not have LFV contributions due to the conservation of Z_3 charge of A_4 and only flavor diagonal contributions like muon $g-2$ may be allowed. The non-zero LFV contributions through lepton transition magnetic moments require the Z_3 symmetry violation, that is, the η VEV. They can arise at one-loop level through mediators, ν_R and N_i $(i = 4, 5, 6))$, but they face the significant suppression due to the small $v_\eta/\Lambda \ll 1$. The LFV process with no chirality flips through Z boson couplings is also aligned to diagonal form due to A_4 symmetry nature $Y_\nu Y_\nu^\dagger = 3\mathrm{diag}((y_\nu^e)^2, (y_\nu^\mu)^2, (y_\nu^\tau)^2)$ if v_η is not picked up, and it is suppressed again as well as the case of the magnetic moment type LFV processes. In this model, A_4 symmetry remains as an approximately good symmetry at low energy and it plays a key role to suppress LFV processes in nature.[14] This is a contrast to the case of only very heavy right-handed Majorana neutrinos added to Standard Model particles where such flavor symmetry may not necessarily play any role to explain the tiny LFV.

[13] As we know in MSSM, if we introduce new scalars with the same SM gauge quantum numbers of right-handed sleptons, we expect the sizable contribution to, for example, muon $g-2$. However, in this case, the annihilation process of ν_R^a can have S-wave component and may have different implications to the relic density and the indirect detection. On the other hand, if the new scalars are A_4 charged and do not acquire VEVs, LFV may be suppressed by A_4 symmetric nature as we will see below.

[14] Even though we add other explicit A_4 breaking terms, this statement may be correct as long as the couplings of added A_4 breaking are small.

JHEP10(2014)183

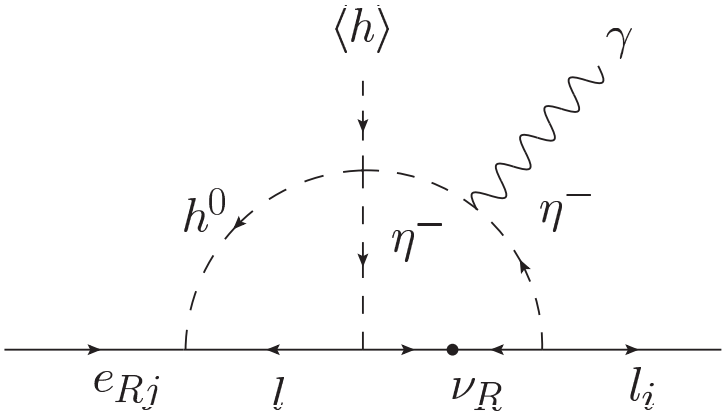

Figure 15. A two loop diagram contributing to lepton transition magnetic moments.

At the last of this section, we consider constraints on N_i $(i = 4, 5, 6)$. The mass scale of these particles are rather free and only the combination of the masses and neutrino Yukawa couplings Y_i $(i = 4, 5, 6)$ are constrained by neutrino masses as the case of usual seesaw mechanism. If we assume TeV-scale N_i $(i = 4, 5, 6)$, the lifetime is $O(1) \times 10^{-14}\text{sec} \times (m_{N_i}/1\text{TeV})^{-1}$. This production at collider may be minor if the mass is heavier than SM Higgs mass. On the other hand, in early universe, it may play some roles at the freeze out time of dark matter or the later, e.g. diluting dark matter relic at late time. Thus we simply assume that they have heavy masses, for example, $\sim 10^{12-13}$GeV.

5 Conclusion and discussion

In this paper, we discussed the discrete dark matter model originally introduced in [15, 16] and showed that this type of models can explain current experimental results of neutrino masses and mixing angles, that is, it can achieve non-zero θ_{13}. We find that this model predicts one relation among neutrino mass matrix elements and the non-zero θ_{13} requires non-zero δs_{23} and m_1 in both NH and IH cases assuming no CP phases. Such prediction can be tested in several future neutrino experiments and cosmological observations. Next, we investigated the possibility of ν_R dark matter, especially focusing on the case that they obtain the desired relic density of observed dark mater. This motivates the existence of TeV-scale ν_R. We could realize such a possibility by introducing an explicit A_4 breaking bilinear term. We find that the current experimental constraints still allow the scenario that the thermal freeze out of ν_R dark matter obtains the desired relic density. Future collider experiments such as the LHC and the ILC may discover the signals or exclude the large parts of interesting parameter spaces. Within TeV-scale ν_R scenario, the A_4 symmetry plays an interesting role to hide LFV processes in low energy physics. We demonstrated that even the two loop processes can be hidden due to the symmetry, and LFV processes only appear when the breaking is picked up, which is highly suppressed by the mismatch of v_η and cut off scale $\gtrsim m_\eta$. This is a contrast to heavy right-handed neutrino scenarios in the role of flavor symmetry.

JHEP10(2014)183

In this paper, we only considered the possibility of TeV-scale ν_R though, notice that the TeV-scale mass is required when we assume that the thermal freeze out obtain the desired relic density of the present dark matter. The physical mass of η is not related to the EW symmetry breaking scale any more thanks to the soft term $m^2_{h\eta_1} h^\dagger \eta$ and the A_4 symmetric η mass term $m^2_\eta \eta^\dagger \eta$. Even in the case that ν_R significantly heavier than 1TeV, we could realize that the η is heavier than ν_R. If we relax the constraints on thermal freeze out for the observed dark matter density, heavy ν_R, e.g stable 10^{12}GeV right-handed neutrinos may be allowed and may obtain other possibilities within the ν_R dark matter scenario, e.g. possibilities of the simultaneous production of dark matter and baryon asymmetry, which was not discussed in this paper. For such heavy ν_R, $m^2_{h\eta}/m^2_\eta$ is not necessarily very small and the small neutrino masses are achieved in the usual meaning of Type I seesaw mechanism. On the other hand, the EW symmetry breaking may require a fine tuning among m^2_h, $m^2_{h\eta}$, and m^2_η at the EW scale, which may be theoretical challenges in different points of view from the case of TeV-scale ν_R.[15] The most of our phenomenological discussions presented in this paper depend on only v_η/Λ. By fixing the ratio, we may find similar conclusions except for the testability in collider experiments.

Acknowledgments

This work is supported in part by the Grant-in-Aid for Scientific Research No. 25400252 (T. K.), No. 23104011 (Y. O.), No.25.1146 (A. O.), No25.1107 (Y. H.) from the Ministry of Education, Culture, Sports, Science and Technology of Japan.

A A short glance at A_4 group

A_4 is the group of even permutation of four objects. In this appendix, we show some properties of A_4 which is needed to describe the discrete dark matter model.

A_4 has four irreducible representations $\mathbf{1}, \mathbf{1}', \mathbf{1}'', \mathbf{3}$, and is generated by two generators S, T which satisfy

$$S^2 = T^3 = 1, \quad (ST)^3 = 1. \tag{A.1}$$

On the trivial singlet $\mathbf{1}$, S and T are represented by $S = 1$ and $T = 1$. $\mathbf{1}'(\mathbf{1}'')$ corresponds to $S = 1, T = \omega(\omega^2)$. Here, ω is a primitive cube root of 1, say $e^{2\pi i/3}$. On $\mathbf{3}$ representation, S and T is represented by

$$S = \begin{pmatrix} 1 & 0 & 0 \\ 0 & -1 & 0 \\ 0 & 0 & -1 \end{pmatrix}, \quad T = \begin{pmatrix} 0 & 1 & 0 \\ 0 & 0 & 1 \\ 1 & 0 & 0 \end{pmatrix}. \tag{A.2}$$

The sub group of A_4 generated by S is left as the symmetry of the discrete dark matter model even after the scalar fields get VEVs. This subgroup Z_2 guarantees stability of a

[15] See the scalar boson spectrum and the condition for the EW symmetry breaking in appendix A.

JHEP10(2014)183

dark matter candidate. Multiplication rule is as below,

$$\begin{aligned}
&\mathbf{1}' \otimes \mathbf{1}' = \mathbf{1}'', \quad \mathbf{1}'' \otimes \mathbf{1}'' = \mathbf{1}', \quad \mathbf{1}' \otimes \mathbf{1}'' = \mathbf{1}, \\
&\mathbf{3} \otimes \mathbf{3} = \mathbf{3}_1 \oplus \mathbf{3}_2 \oplus \mathbf{1} \oplus \mathbf{1}' \oplus \mathbf{1}''.
\end{aligned} \tag{A.3}$$

For example, when $a = (a_1, a_2, a_3)$ and $b = (b_1, b_2, b_3)$ are two A_4 triplets, the ways to compose $\mathbf{1}, \mathbf{1}', \mathbf{1}''$ and $\mathbf{3}$ representation from them are

$$\begin{aligned}
(ab)_{\mathbf{1}} &= a_1 b_1 + a_2 b_2 + a_3 b_3, \\
(ab)_{\mathbf{1}'} &= a_1 b_1 + \omega a_2 b_2 + \omega^2 a_3 b_3, \\
(ab)_{\mathbf{1}''} &= a_1 b_1 + \omega^2 a_2 b_2 + \omega a_3 b_3, \\
(ab)_{\mathbf{3}_1} &= \begin{pmatrix} a_2 b_3 \\ a_3 b_1 \\ a_1 b_2 \end{pmatrix}, \quad (ab)_{\mathbf{3}_2} = \begin{pmatrix} a_3 b_2 \\ a_1 b_3 \\ a_2 b_1 \end{pmatrix}.
\end{aligned} \tag{A.4}$$

B Scalar boson potential and the physical spectrum

General form of CP and A_4 invariant potential terms of scalar bosons are given by,

$$\begin{aligned}
V(h,\eta) = {} & m_\eta^2 \eta^\dagger \eta + m_h^2 h^\dagger h \\
& + \lambda_1 (h^\dagger h)^2 + \lambda_2 [\eta^\dagger \eta]_1^2 + \lambda_3 [\eta^\dagger \eta]_{1'} [\eta^\dagger \eta]_{1''} \\
& + \lambda_4 ([\eta^\dagger \eta^\dagger]_{1'} [\eta\eta]_{1''} + [\eta^\dagger \eta^\dagger]_{1''} [\eta\eta]_{1'}) + \lambda_5 [\eta^\dagger \eta^\dagger]_1 [\eta\eta]_1 \\
& + \lambda_6 ([\eta^\dagger \eta]_{3_1} [\eta^\dagger \eta]_{3_1} + [\eta^\dagger \eta]_{3_2} [\eta^\dagger \eta]_{3_2}) + \lambda_7 [\eta^\dagger \eta]_{3_1} [\eta^\dagger \eta]_{3_2} + \lambda_8 [\eta^\dagger \eta^\dagger]_{3_1} [\eta\eta]_{3_1} \\
& + \lambda_9 [\eta^\dagger \eta]_1 (h^\dagger h) + \lambda_{10} [\eta^\dagger h]_3 [h^\dagger \eta]_3 + \lambda_{11} ([\eta^\dagger \eta^\dagger]_1 hh + h^\dagger h^\dagger [\eta\eta]_1) \\
& + \lambda_{12} ([\eta^\dagger \eta^\dagger]_{3_1} [\eta h]_3 + [h^\dagger \eta^\dagger]_3 [\eta\eta]_{3_2}) + \lambda_{13} ([\eta^\dagger \eta^\dagger]_{3_2} [\eta h]_3 + [h^\dagger \eta^\dagger]_3 [\eta\eta]_{3_1}) \\
& + \lambda_{14} ([\eta^\dagger \eta]_{3_1} [\eta^\dagger h]_3 + [h^\dagger \eta]_3 [\eta^\dagger \eta]_{3_2}) + \lambda_{15} ([\eta^\dagger \eta]_{3_2} [\eta^\dagger h]_3 + [h^\dagger \eta]_3 [\eta^\dagger \eta]_{3_1}).
\end{aligned} \tag{B.1}$$

To explain observed tiny neutrino masses in our scenario, we have to demand smallness for $m_{h\eta_1}^2$ and λ_{11}. The quantum corrections due to $\Delta\eta = 1$ interactions, λ_{12}, λ_{13}, λ_{14} and λ_{15} generate λ_{11} at one loop, so these conpligs also have to be suppressed $< m_{h\eta_1}^2/m_\eta^2$. This may exhibit an approximate global $\mathrm{U}(1)_\eta$ symmetry in the scalar potential. Notice that λ_{11} also violates $\mathrm{U}(1)_\eta$ by $\Delta\eta = 2$ but the quantum corrections by itself never generate $\Delta\eta = 1$ interactions.

As we mentioned in section 2, we add the following A_4 explicit breaking term,

$$V_{\mathrm{soft}} = -m_{h\eta_1}^2 \eta_1^\dagger h + \mathrm{h.c.}, \tag{B.2}$$

which explicitly breaks $\mathrm{U}(1)_\eta$ by $\Delta\eta = 1$.

We notice that in this scalar potential, an exact invariance for an odd permutation between η_2 and η_3 exists. The full invariance for all three odd permutations among η_1, η_2 and η_3 recovers if we ignore the soft term $m_{h\eta_1}^2$. The (η_2, η_3) permutation is not a symmetry inside A_4 symmetry but an accidental symmetry in our model when we impose

JHEP10(2014)183

CP invariance in scalar potential. As we explain in appendix D, this invariance for (η_2, η_3) permutation is crucial to obtain a relation of eq. (3.8) in neutrino mass matrix elements. CP invariance in all couplings of the scalar potential is not always nesessary for the invariance of (η_2, η_3) odd permutation in scalar potential, for example, the CP invariance in λ_{11} coupling can be relaxed for this purpose. The phase of λ_{11} can introduce CP phases for neutrino mass matrix without changing the relation eq. (3.8). In general, inclusions of CP phases in the other terms of scalar potential may violate the invariance for (η_2, η_3) permutation, for example, by the following term,

$$\lambda_4[\eta^\dagger\eta^\dagger]_{1'}[\eta\eta]_{1''} + \lambda_{4'}[\eta^\dagger\eta^\dagger]_{1''}[\eta\eta]_{1'}, \tag{B.3}$$

where $\lambda_4 \neq \lambda_{4'}$. In such cases, the relation eq. (3.8) is not hold any more, which results more freedom to describe neutrino mass matrix in this model.

We expand the fields around the physical vacuum $\langle h\rangle = v_h$, $(\langle\eta_1\rangle, \langle\eta_2\rangle, \langle\eta_3\rangle) = (v_\eta, 0, 0)$,

$$h = \begin{pmatrix} h^+ \\ v_h + h^0 + iA_h^0 \end{pmatrix},\ \eta_1 = \begin{pmatrix} \eta_1^+ \\ v_\eta + \eta_1^0 + iA_{\eta_1}^0 \end{pmatrix},\ \eta_{2,3} = \begin{pmatrix} \eta_{2,3}^+ \\ \eta_{2,3}^0 + iA_{\eta_{2,3}}^0 \end{pmatrix}. \tag{B.4}$$

We define new couplings as follows [16],

$$L = \lambda_9 + \lambda_{10} + 2\lambda_{11}, \tag{B.5}$$
$$Q = \lambda_{12} + \lambda_{13} + \lambda_{14} + \lambda_{15}, \tag{B.6}$$
$$P = \lambda_2 + \lambda_3 + 2\lambda_4 + \lambda_5, \tag{B.7}$$
$$R_1 = -3\lambda_3 - 6\lambda_4 + 2\lambda_6 + \lambda_7 + \lambda_8, \tag{B.8}$$
$$R_2 = -3\lambda_3 - 2\lambda_4 - 4\lambda_5 - 2\lambda_6 + \lambda_7 + \lambda_8, \tag{B.9}$$
$$R_3 = -3\lambda_3 - 4\lambda_4 - 2\lambda_5 + \lambda_8. \tag{B.10}$$

Then the minimalization conditions for scalar potential are written by,

$$m_h^2 + 2\lambda_1 v_h^2 + Lv_\eta^2 - m_{h\eta}^2\frac{v_\eta}{v_h} = 0, \tag{B.11}$$
$$m_\eta^2 + 2Pv_\eta^2 + Lv_h^2 - m_{h\eta}^2\frac{v_h}{v_\eta} = 0. \tag{B.12}$$

From the second condition, we approximately read $v_\eta \sim \frac{m_{h\eta_1}^2}{m_\eta^2}v_h$ when $m_{h\eta_1}^2/m_\eta^2 \ll 1$.

B.1 Physical spectrum of scalar bosons

The physical states of Z_2 even and parity even charged Higgs boson sector are

$$h_0^+ = \frac{v_h}{v}h^+ - \frac{v_\eta}{v}\eta^+,\ h_1^+ = \frac{v_\eta}{v}h^+ + \frac{v_h}{v}\eta^+, \tag{B.13}$$

where $v = \sqrt{v_h^2 + v_\eta^2}$. The physical mass spectrum is obtained as

$$m_{h_0^+}^2 = 0,\ m_{h_1^+}^2 = (\frac{m_{h\eta}^2}{v_h v_\eta} - \lambda_{10} - \lambda_{11})v^2. \tag{B.14}$$

The physical states of Z_2 even and parity even neutral Higgs boson sector are,

$$h_0^0 = h^0\cos\phi - \eta_1^0\sin\phi,\ h_1^0 = h^0\sin\phi + \eta_1^0\cos\phi, \tag{B.15}$$

JHEP10(2014)183

where the mixing angle is

$$\tan 2\phi = \frac{2Lv_\eta v_h + m_{h\eta}^2}{2Pv_\eta^2 - 2\lambda_1 v_h^2 - \frac{m_{h\eta}^2}{2}\left(\frac{v_h}{v_\eta} - \frac{v_\eta}{v_h}\right)}, \tag{B.16}$$

and the mass spectrum is written by

$$m_{h_{0,1}}^2 = 2\lambda_1 v_h^2 + 2Pv_\eta^2 + \frac{m_{h\eta}^2}{2v_h v_\eta}v^2 \pm \sqrt{\left(2\lambda_1 v_h^2 - 2Pv_\eta^2 - \frac{m_{h\eta}^2}{2v_h v_\eta}(v_h^2 - v_\eta^2)\right)^2 + \left(2L - \frac{m_{h\eta}^2}{v_h v_\eta}\right)^2 v_h^2 v_\eta^2}. \tag{B.17}$$

The physical states of Z_2 even and parity odd neutral pseudo scalar Higgs boson sector are

$$A_0^0 = \frac{v_h}{v}A_h^0 - \frac{v_\eta}{v}A_{\eta_1}^0,\ A_1^0 = \frac{v_\eta}{v}A_h^0 + \frac{v_h}{v}A_{\eta_1}^0, \tag{B.18}$$

and the mass spectrum is written by

$$m_{A_0}^2 = 0,\ m_{A_1}^2 = (\frac{m_{h\eta}^2}{v_h v_\eta} - 4\lambda_{11})v^2. \tag{B.19}$$

The physical states of Z_2 odd and parity even charged Higgs boson sector are,

$$h_2^+ = \frac{1}{\sqrt{2}}(\eta_2^+ - \eta_3^+),\ h_3^+ = \frac{1}{\sqrt{2}}(\eta_2^+ + \eta_3^+), \tag{B.20}$$

and the mass spectrum is written by,

$$m_{h_{2,3}^+}^2 = R_3 v_\eta^2 - (\lambda_{10} + 2\lambda_{11})v_h^2 + m_{h\eta}^2\frac{v_h}{v_\eta} \pm Qv_h v_\eta. \tag{B.21}$$

The physical states of Z_2 odd and parity even neutral Higgs boson are,

$$h_2^0 = \frac{1}{\sqrt{2}}(\eta_2^0 - \eta_3^0),\ h_3^0 = \frac{1}{\sqrt{2}}(\eta_2^0 + \eta_3^0), \tag{B.22}$$

and the mass spectrum is written by,

$$m_{h_{2,3}}^2 = R_1 v_\eta^2 + m_{h\eta}^2\frac{v_h}{v_\eta} \pm Qv_h v_\eta. \tag{B.23}$$

The physical sates of Z_2 odd and parity odd neutral Higgs boson are,

$$A_2^0 = \frac{1}{\sqrt{2}}(A_{\eta_2}^0 - A_{\eta_3}^0),\ A_3^0 = \frac{1}{\sqrt{2}}(A_{\eta_2}^0 + A_{\eta_3}^0), \tag{B.24}$$

and the mass spectrum is written by,

$$m_{A_{2,3}}^2 = R_2 v_\eta^2 - 4\lambda_{11}v_h^2 + m_{h\eta}^2\frac{v_h}{v_\eta} \pm Qv_h v_\eta. \tag{B.25}$$

We find that the zero mass states are absorbed into the longitudinal components of electroweak massive gauge bosons.

JHEP10(2014)183

C Neutrino mass matrix and the prediction of discrete dark matter models

Using the conventional form for PMNS matrix in eq. (3.10), we can relate the neutrino mass matrix elements to the observed masses and mixing parameters as follow,

$$(m_\nu) = U_{\rm PMNS} \begin{pmatrix} |m_1| & 0 & 0 \\ 0 & |m_2| & 0 \\ 0 & 0 & |m_3| \end{pmatrix} U^T_{\rm PMNS} = \begin{pmatrix} (m_\nu)_{11} & (m_\nu)_{12} & (m_\nu)_{13} \\ (m_\nu)^*_{12} & (m_\nu)_{22} & (m_\nu)_{23} \\ (m_\nu)^*_{13} & (m_\nu)^*_{23} & (m_\nu)_{33} \end{pmatrix}, \quad \text{(C.1)}$$

$$\begin{aligned}
(m_\nu)_{11} &= c^2_{13}(m_1 c^2_{12} + s^2_{12} m_2) + s^2_{13} m_3, && \text{(C.2)}\\
(m_\nu)_{22} &= -2 s_{12} c_{12} s_{23} c_{23} s_{13} \delta m_{12} \cos\delta \\
&\quad + c^2_{23}(s^2_{12} m_1 + c^2_{12} m_2) + s^2_{23} s^2_{13}(c^2_{12} m_1 + s^2_{12} m_2) + s^2_{23} c^2_{13} m_3, && \text{(C.3)}\\
(m_\nu)_{33} &= 2 s_{12} c_{12} s_{23} c_{23} s_{13} \delta m_{12} \cos\delta \\
&\quad + s^2_{23}(s^2_{12} m_1 + c^2_{12} m_2) + c^2_{23} s^2_{13}(c^2_{12} m_1 + s^2_{12} m_2) + c^2_{23} c^2_{13} m_3, && \text{(C.4)}\\
(m_\nu)_{12} &= s_{12} c_{12} c_{23} c_{13} \delta m_{12} - s_{23} s_{13} c_{13} e^{-i\delta}(c^2_{12} m_1 + s^2_{12} m_2 - m_3), && \text{(C.5)}\\
(m_\nu)_{13} &= -s_{12} c_{12} s_{23} c_{13} \delta m_{12} - c_{23} s_{13} c_{13} e^{-i\delta}(c^2_{12} m_1 + s^2_{12} m_2 - m_3), && \text{(C.6)}\\
(m_\nu)_{23} &= s_{12} c_{12} s_{13}(s^2_{23} e^{i\delta} - c^2_{23} e^{-i\delta}) \delta m_{12} \\
&\quad - s_{23} c_{23} \left((s^2_{12} m_1 + c^2_{12} m_2) - s^2_{13}(c^2_{12} m_1 + c^2_{12} m_2)\right) + s_{23} c_{23} c^2_{13} m_3, \\
& && \text{(C.7)}
\end{aligned}$$

where the masses are defined as $m_1 = |m_1|$, $m_2 = |m_2| e^{i\phi_2}$ and $m_3 = |m_3| e^{i\phi_3}$.

We can find the following structure for $(m_\nu)_{12}$, $(m_\nu)_{13}$, $(m_\nu)_{22}$ and $(m_\nu)_{33}$,

$$\begin{aligned}
(m_\nu)_{22} &= -A s_{23} c_{23} + B c^2_{23} + C s^2_{23}, && \text{(C.8)}\\
(m_\nu)_{33} &= A s_{23} c_{23} + B s^2_{23} + C c^2_{23}, && \text{(C.9)}\\
(m_\nu)_{12} &= X c_{23} - Y s_{23}, && \text{(C.10)}\\
(m_\nu)_{13} &= -X s_{23} - Y c_{23}, && \text{(C.11)}
\end{aligned}$$

$$\begin{aligned}
A &= 2 s_{12} c_{12} s_{13} \delta m_{12} \cos\delta, && \text{(C.12)}\\
B &= (s^2_{12} m_1 + c^2_{12} m_2), && \text{(C.13)}\\
C &= s^2_{13}(c^2_{12} m_1 + s^2_{12} m_2) + c^2_{13} m_3, && \text{(C.14)}\\
X &= s_{12} c_{12} c_{13} \delta m_{12}, && \text{(C.15)}\\
Y &= s_{13} c_{13} e^{-i\delta}((c^2_{12} m_1 + s^2_{12} m_2) - m_3). && \text{(C.16)}
\end{aligned}$$

Our discrete dark matter model predicts eq. (3.8). The condition $(m_\nu)^2_{12}/(m_\nu)_{22} = (m_\nu)^2_{13}/(m_\nu)_{33}$ gives

$$\begin{aligned}
\frac{1}{\tan(2\theta_{23})} &= \frac{1}{2} \times \frac{A(X^2 + Y^2) - 2(B + C)XY}{BY^2 - CX^2}, && \text{(C.17)}\\
s_{23} &= \sin(\frac{\arctan(2\theta_{23})}{2}). && \text{(C.18)}
\end{aligned}$$

JHEP10(2014)183

Notice that $A \propto \delta m_{12} s_{13} s_{12}$, $X \propto \delta m_{12} s_{12}$ and $Y \propto s_{13}$. Then we find that the right hand side of eq. (C.17) is,

$$\frac{A(X^2+Y^2) - 2(B+C)XY}{BY^2 - CX^2} \propto \delta m_{12} s_{13} s_{12}. \tag{C.19}$$

If we take $s_{13} = 0$, then $c_{23}^2 = s_{23}^2 = 1/2$ is required and Tri-bimaximal mass pattern taken in original paper [15, 16] can be realized. On the other hand, if we take non-zero s_{13}, in general, δs_{23} is proportional to δm_{12}. Since the observed δm_{12} is not zero, we can expect non-zero deviation δs_{23} from $s_{23}^2 = 1/2$.

For $m_i > 0$ $(i = 1, 2, 3)$ and degenerate spectrum, we obtain $\delta m_{12} \ll m_1$. Then we obtain $CX^2 \ll BY^2$ even in the case of small $s_{13} \sim 0.15$. In such a case, we find the approximate formula presented as eq. (3.14).

In the case of real m_1, m_2 and m_3, the imaginary part of the condition eq. (3.9) obtain

$$\begin{aligned}([-A(c_{12}^2 m_1 + s_{12}^2 m_2 - m_3) s_{13} c_{13} \cos\delta + (B+C)X] s_{23} c_{23} \\ + B(c_{12}^2 m_1 + s_{12}^2 m_2 - m_3)(c_{23}^2 - s_{23}^2) s_{13} c_{13} \cos\delta) \sin\delta = 0.\end{aligned} \tag{C.20}$$

The possible choice is $\sin\delta = 0$, that is, $\delta = 0, \pi$.

Taking $s_{23} = \mathrm{sgn}(s_{23})/\sqrt{2} + \delta s_{23}$, for the cases of no CP phases, the following relation among neutrino masses and mixing parameters is derived,

$$\delta s_{23} = \frac{(s_{12} s_{13}/2\sqrt{2}) \delta m_{12} (m_1 m_2 - (c_{12}^2 - s_{12}^2) \delta m_{12} m_3 - m_3^2)}{(s_{12}^2 c_{12}^2 [s_{13}^2 (c_{12}^2 m_1 + s_{12}^2 m_2) + c_{13}^2 m_3](\delta m_{12})^2 - s_{13}^2 (s_{12}^2 m_1 + c_{12}^2 m_2)(c_{12}^2 m_1 + s_{12}^2 m_2 - m_3)^2)}. \tag{C.21}$$

D Radiatively induced neutrino mass structure in discrete dark matter model

As we mentioned in section 3, the model can generate neutrino masses through radiative correction at loop level. Here we explain that the radiative corrections induce the mass structure described in section 3. Since η boson is almost diagonal in mass, here we take mass insertion approximation.

At one loop, the flavor mixing of ν_Rs is highly suppressed at the order of $(v_\eta/m_\eta)^2$ or higher order. This requires that the η boson propagating inside the loop diagram can not change the flavor indices to connect with internal ν_R line. Another restriction comes from the special pattern of η VEVs $(\langle\eta_1\rangle, \langle\eta_2\rangle, \langle\eta_3\rangle) = (v_\eta, 0, 0)$.

The first type arises through λ_{11} coupling(See figure3.). In this case, the η propagating internal line of the loop has universal couplings for all the indices $(i = 1, 2, 3)$ in the four points scalar interactions. The $\mathrm{SU(2)_L}$ breaking in neutrino masses happens through two v_h and there is no A_4 breaking part in this diagram at the leading piece. This type obtains A_4 symmetric mass structure m^{sym}. That is, the non zero pieces are

$$(m_\nu)_{11}^{\mathrm{rad:1}} = \lambda_{11} y_\nu^e y_\nu^e \frac{v_h^2}{m_N} f(m_\eta, m_N), \tag{D.1}$$

$$(m_\nu)_{23}^{\mathrm{rad:1}} = (m_\nu)_{32}^{\mathrm{rad:1}} = \lambda_{11} y_\nu^\mu y_\nu^\tau \frac{v_h^2}{m_N} f(m_\eta, m_N), \tag{D.2}$$

JHEP10(2014)183

where $f(x,y) \sim \frac{1}{16\pi^2}\frac{y^2}{x^2-y^2}[\frac{y^2}{x^2-y^2}][\log(\frac{x^2}{y^2})+1]$ is a loop function. We used $\lambda_{11}v_\eta^2 \ll (m_\eta^2 - m_N^2)$.

The second type arises through λ_4 and λ_5 couplings(See figure1.). In this case, both two of ηs acquire the VEV and the two η bosons constitute singlets $(1, 1', 1'')$, we find that the common piece of η_2 and η_3 loop vanishes due to Z_3 nature $1+\omega+\omega^2=0$ and the mismatch of the two couplings, $\lambda_5 - \lambda_4$ allows the non zero contributions for η_2 and η_3 loops. As a result, we find two mass structures. The first one is A_4 symmetric mass structure $m^{\rm sym}$ which is proportinal to $\lambda_5 - \lambda_4$,

$$(m_\nu)_{11}^{\rm rad:2,sym} = (\lambda_5-\lambda_4)y_\nu^e y_\nu^e \frac{v_\eta^2}{m_N} f(m_\eta, m_N), \tag{D.3}$$

$$(m_\nu)_{23}^{\rm rad:2,sym} = (m_\nu)_{32}^{\rm rad:1} = (\lambda_5-\lambda_4)y_\nu^\mu y_\nu^\tau \frac{v_\eta^2}{m_N} f(m_\eta, m_N), \tag{D.4}$$

and the second one is A_4 violating mass structure $m^{\rm break}$ which is proportional to $3\lambda_4$,

$$(m_\nu)_{ij}^{\rm rad:2,break} = 3\lambda_4 y_\nu^i y_\nu^j \frac{v_\eta^2}{m_N} f(m_\eta, m_N). \tag{D.5}$$

The third type arises through λ_2 and λ_3 couplings. In this case, the η constitute singlets with the η propagating internal line in the loop. Since only η_1 acquire non zero VEV, only η_1 can be allowed to propagate the internal line which results the same mass pattern given in the type I tree level seesaw contribution, that is, A_4 violating mass structure, $m^{\rm break}$,

$$(m_\nu)_{ij}^{\rm rad:3,break} = 3(\lambda_2+\lambda_3)y_\nu^i y_\nu^j \frac{v_\eta^2}{m_N} f(m_\eta, m_N). \tag{D.6}$$

The forth type is induced through λ_6 coupling. In this case, only η_2 and η_3 are allowed to propagate the internal line of loops. Then we find that this contribution is regarded as the sum of $m^{\rm sym}$,

$$(m_\nu)_{11}^{\rm rad:4,sym} = \lambda_6 y_\nu^e y_\nu^e \frac{v_\eta^2}{m_N} f(m_\eta, m_N), \tag{D.7}$$

$$(m_\nu)_{23}^{\rm rad:4,sym} = (m_\nu)_{32}^{\rm rad:4} = \lambda_6 y_\nu^\mu y_\nu^\tau \frac{v_\eta^2}{m_N} f(m_\eta, m_N), \tag{D.8}$$

and $m^{\rm break}$,

$$(m_\nu)_{ij}^{\rm rad:4,break} = -\lambda_6 y_\nu^i y_\nu^j \frac{v_\eta^2}{m_N} f(m_\eta, m_N). \tag{D.9}$$

The contributions from $\Delta\eta = 1$ interactions pick up two $\Delta\eta = 1$ couplings and two η vevs. They obtain negligible contributions becuase of the smallness of $\Delta\eta = 1$ couplings. $\Delta\eta = 2$ coupling λ_{11} can also contribute to $m^{\rm break}$ by picking up η vev and it is also significantly small and negligible.

Correcting above all contributions, we find that neutrino mass in our model can be described by the two types of mass structure, $m^{\rm sym}$ and $m^{\rm break}$.

JHEP10(2014)183

As we mentioned in appendix B, under our A_4 breaking pattern, the invariance for (η_2, η_3) permutation in scalar potential is crucial to have the special pattern of $m^{\rm break}$ given in eq. (3.4), that is, to obtain the relation eq. (3.8). This can be easily seen as follows. Here notice that our lagragian is invariant for an exchange of $(\eta_2, N_2, (y_\nu^\mu, L_\mu), (y_\mu, \mu_R))$ and $(\eta_3, N_3, (y_\nu^\tau, L_\tau), (y_\tau, \tau_R))$.[16] In loop diagrams contributing to neutrino masses, we see that fixing the flavors of external two leptons, the amplitudes except for the two vertex with fixed external leptons are invariant against the exchange. The entanglements for the permutation at the two vertex is disentangled by $((y_\nu^\mu, L_\mu), (y_\nu^\eta, L_\tau))$ exchange in the external leptons. As the result, the invariance of scalar potential for (η_2, η_3) permutation demands the universality for the coefficients of the follwoing two Dim 5 neutrino mass operators,

$$\frac{1}{\Lambda_a}[(y_\nu^\alpha L)(y_\nu^\beta L)]_{1'}[(\eta^\dagger \eta^\dagger)]_{1''}\,,\ \frac{1}{\Lambda_b}[(y_\nu^\alpha L)(y_\nu^\beta L)]_{1''}[(\eta^\dagger \eta^\dagger)]_{1'}\,, \tag{D.10}$$

that is, $\Lambda_a = \Lambda_b$. This universality of the cut-off scale results the relation eq. (3.8). The relation of eq. (3.8) is stable against the extentions of models as long as the lagragian is invariant for (η_2, η_3) permutation.

If the invariance for (η_2, η_3) permutation is lost, e.g by introduing CP phases in scalar potential, since we can not expect a relation such as $\Lambda_a = \Lambda_b$, the expression for $m^{\rm break}$ is not valid any more and the relation among neutrino mass parameters as Eq. (3.8) is lost, which means that we have more freedom to explain neutrino mass.

Open Access. This article is distributed under the terms of the Creative Commons Attribution License (CC-BY 4.0), which permits any use, distribution and reproduction in any medium, provided the original author(s) and source are credited.

References

[1] P.F. Harrison, D.H. Perkins and W.G. Scott, *Tri-bimaximal mixing and the neutrino oscillation data*, *Phys. Lett.* **B 530** (2002) 167 [hep-ph/0202074] [INSPIRE].

[2] P.F. Harrison and W.G. Scott, *Symmetries and generalizations of tri - bimaximal neutrino mixing*, *Phys. Lett.* **B 535** (2002) 163 [hep-ph/0203209] [INSPIRE].

[3] P.F. Harrison and W.G. Scott, *Permutation symmetry, tri - bimaximal neutrino mixing and the S3 group characters*, *Phys. Lett.* **B 557** (2003) 76 [hep-ph/0302025] [INSPIRE].

[4] DAYA-BAY collaboration, F.P. An et al., *Observation of electron-antineutrino disappearance at Daya Bay*, *Phys. Rev. Lett.* **108** (2012) 171803 [arXiv:1203.1669] [INSPIRE].

[5] DAYA BAY collaboration, F.P. An et al., *Improved Measurement of Electron Antineutrino Disappearance at Daya Bay*, *Chin. Phys.* **C 37** (2013) 011001 [arXiv:1210.6327] [INSPIRE].

[6] DOUBLE-CHOOZ collaboration, Y. Abe et al., *Indication for the disappearance of reactor electron antineutrinos in the Double CHOOZ experiment*, *Phys. Rev. Lett.* **108** (2012) 131801 [arXiv:1112.6353] [INSPIRE].

[16] If we include N_5,, N_6, an exchange of $(\eta_2, N_2, (y_\nu^\mu, L_\mu), (y_\mu, \mu_R), N_5)$ and $(\eta_3, N_3, (y_\nu^\tau, L_\tau), (y_\tau, \tau_R), N_6)$ leaves the lagragian invariant.

JHEP10(2014)183

[7] RENO collaboration, J.K. Ahn et al., *Observation of Reactor Electron Antineutrino Disappearance in the RENO Experiment*, *Phys. Rev. Lett.* **108** (2012) 191802 [arXiv:1204.0626] [INSPIRE].

[8] T2K collaboration, K. Abe et al., *Indication of Electron Neutrino Appearance from an Accelerator-produced Off-axis Muon Neutrino Beam*, *Phys. Rev. Lett.* **107** (2011) 041801 [arXiv:1106.2822] [INSPIRE].

[9] MINOS collaboration, P. Adamson et al., *Improved search for muon-neutrino to electron-neutrino oscillations in MINOS*, *Phys. Rev. Lett.* **107** (2011) 181802 [arXiv:1108.0015] [INSPIRE].

[10] G. Altarelli and F. Feruglio, *Discrete Flavor Symmetries and Models of Neutrino Mixing*, *Rev. Mod. Phys.* **82** (2010) 2701 [arXiv:1002.0211] [INSPIRE].

[11] H. Ishimori, T. Kobayashi, H. Ohki, Y. Shimizu, H. Okada et al., *Non-Abelian Discrete Symmetries in Particle Physics*, *Prog. Theor. Phys. Suppl.* **183** (2010) 1 [arXiv:1003.3552] [INSPIRE].

[12] H. Ishimori, T. Kobayashi, H. Ohki, H. Okada, Y. Shimizu and M. Tanimoto, *An introduction to non-Abelian discrete symmetries for particle physicists*, *Lect. Notes Phys.* **858** (2012) 1.

[13] H. Ishimori, T. Kobayashi, Y. Shimizu, H. Ohki, H. Okada et al., *Non-Abelian discrete symmetry for flavors*, *Fortsch. Phys.* **61** (2013) 441 [INSPIRE].

[14] S.F. King and C. Luhn, *Neutrino Mass and Mixing with Discrete Symmetry*, *Rept. Prog. Phys.* **76** (2013) 056201 [arXiv:1301.1340] [INSPIRE].

[15] M. Hirsch, S. Morisi, E. Peinado and J.W.F. Valle, *Discrete dark matter*, *Phys. Rev.* **D 82** (2010) 116003 [arXiv:1007.0871] [INSPIRE].

[16] M.S. Boucenna, M. Hirsch, S. Morisi, E. Peinado, M. Taoso et al., *Phenomenology of Dark Matter from A_4 Flavor Symmetry*, *JHEP* **05** (2011) 037 [arXiv:1101.2874] [INSPIRE].

[17] Y. Kajiyama and H. Okada, *T(13) Flavor Symmetry and Decaying Dark Matter*, *Nucl. Phys.* **B 848** (2011) 303 [arXiv:1011.5753] [INSPIRE].

[18] T. Asaka, S. Blanchet and M. Shaposhnikov, *The nuMSM, dark matter and neutrino masses*, *Phys. Lett.* **B 631** (2005) 151 [hep-ph/0503065] [INSPIRE].

[19] D. Meloni, S. Morisi and E. Peinado, *Stability of dark matter from the D4xZ2 flavor group*, *Phys. Lett.* **B 703** (2011) 281 [arXiv:1104.0178] [INSPIRE].

[20] Y. Kajiyama, H. Okada and T. Toma, *Direct and Indirect Detection of Dark Matter in D6 Flavor Symmetric Model*, *Eur. Phys. J.* **C 71** (2011) 1688 [arXiv:1104.0367] [INSPIRE].

[21] M.S. Boucenna, S. Morisi, E. Peinado, Y. Shimizu and J.W.F. Valle, *Predictive discrete dark matter model and neutrino oscillations*, *Phys. Rev.* **D 86** (2012) 073008 [arXiv:1204.4733] [INSPIRE].

[22] M.S. Boucenna, S. Morisi, E. Peinado, Y. Shimizu and J.W.F. Valle, *Predictive discrete dark matter model and neutrino oscillations*, *Phys. Rev.* **D 86** (2012) 073008 [arXiv:1204.4733] [INSPIRE].

[23] D. Meloni, S. Morisi and E. Peinado, *Neutrino phenomenology and stable dark matter with A4*, *Phys. Lett.* **B 697** (2011) 339 [arXiv:1011.1371] [INSPIRE].

JHEP10(2014)183

[24] Y.H. Ahn, S.K. Kang and C.S. Kim, *Spontaneous CP-violation in A_4 Flavor Symmetry and Leptogenesis*, *Phys. Rev.* **D 87** (2013) 113012 [arXiv:1304.0921] [INSPIRE].

[25] G.L. Fogli, E. Lisi, A. Marrone, D. Montanino, A. Palazzo et al., *Global analysis of neutrino masses, mixings and phases: entering the era of leptonic CP-violation searches*, *Phys. Rev.* **D 86** (2012) 013012 [arXiv:1205.5254] [INSPIRE].

[26] D.V. Forero, M. Tortola and J.W.F. Valle, *Global status of neutrino oscillation parameters after Neutrino-2012*, *Phys. Rev.* **D 86** (2012) 073012 [arXiv:1205.4018] [INSPIRE].

[27] M.C. Gonzalez-Garcia, M. Maltoni, J. Salvado and T. Schwetz, *Global fit to three neutrino mixing: critical look at present precision*, *JHEP* **12** (2012) 123 [arXiv:1209.3023] [INSPIRE].

[28] T2K collaboration, K. Abe et al., *Precise Measurement of the Neutrino Mixing Parameter θ_{23} from Muon Neutrino Disappearance in an Off-axis Beam*, *Phys. Rev. Lett.* **112** (2014) 181801 [arXiv:1403.1532] [INSPIRE].

[29] MINOS collaboration, P. Adamson et al., *Combined analysis of ν_μ disappearance and $\nu_\mu \to \nu_e$ appearance in MINOS using accelerator and atmospheric neutrinos*, *Phys. Rev. Lett.* **112** (2014) 191801 [arXiv:1403.0867] [INSPIRE].

[30] SUPER-KAMIOKANDE collaboration, A. Himmel, *Recent results from Super-Kamiokande*, *AIP Conf. Proc.* **1604** (2014) 345 [arXiv:1310.6677] [INSPIRE].

[31] KAMLAND-ZEN collaboration, A. Gando et al., *Limit on Neutrinoless $\beta\beta$ Decay of Xe-136 from the First Phase of KamLAND-Zen and Comparison with the Positive Claim in Ge-76*, *Phys. Rev. Lett.* **110** (2013) 062502 [arXiv:1211.3863] [INSPIRE].

[32] KAMLAND-ZEN collaboration, A. Gando et al., *Measurement of the double-β decay half-life of ^{136}Xe with the KamLAND-Zen experiment*, *Phys. Rev.* **C 85** (2012) 045504 [arXiv:1201.4664] [INSPIRE].

[33] EXO-200 collaboration, J.B. Albert et al., *Search for Majorana neutrinos with the first two years of EXO-200 data*, *Nature* **510** (2014) 229 [arXiv:1402.6956] [INSPIRE].

[34] PLANCK collaboration, P.A.R. Ade et al., *Planck 2013 results. XVI. Cosmological parameters*, *Astron. Astrophys.* (2014) [arXiv:1303.5076] [INSPIRE].

[35] S.-H. Kim, K.-i. Takemasa, Y. Takeuchi and S. Matsuura, *Search for Radiative Decays of Cosmic Background Neutrino using Cosmic Infrared Background Energy Spectrum*, *J. Phys. Soc. Jap.* **81** (2012) 024101 [arXiv:1112.4568] [INSPIRE].

[36] ATLAS collaboration, *Search for direct production of charginos, neutralinos and sleptons in final states with two leptons and missing transverse momentum in pp collisions at $\sqrt{s} = 8$ TeV with the ATLAS detector*, *JHEP* **05** (2014) 071 [arXiv:1403.5294] [INSPIRE].

[37] CMS Collaboration, *Search for electroweak production of charginos, neutralinos and sleptons using leptonic final states in pp collisions at 8 TeV*, CMS-PAS-SUS-13-006.

[38] L. Bergstrom, T. Bringmann, M. Eriksson and M. Gustafsson, *Gamma rays from Kaluza-Klein dark matter*, *Phys. Rev. Lett.* **94** (2005) 131301 [astro-ph/0410359] [INSPIRE].

[39] A. Birkedal, K.T. Matchev, M. Perelstein and A. Spray, *Robust gamma ray signature of WIMP dark matter*, hep-ph/0507194 [INSPIRE].

[40] T. Bringmann, L. Bergstrom and J. Edsjo, *New Gamma-Ray Contributions to Supersymmetric Dark Matter Annihilation*, *JHEP* **01** (2008) 049 [arXiv:0710.3169] [INSPIRE].

JHEP10(2014)183

[41] M. Asano, T. Bringmann, G. Sigl and M. Vollmann, *130 GeV gamma-ray line and generic dark matter model building constraints from continuum gamma rays, radio and antiproton data*, *Phys. Rev.* **D 87** (2013) 103509 [arXiv:1211.6739] [INSPIRE].

[42] T. Bringmann, X. Huang, A. Ibarra, S. Vogl and C. Weniger, *Fermi LAT Search for Internal Bremsstrahlung Signatures from Dark Matter Annihilation*, *JCAP* **07** (2012) 054 [arXiv:1203.1312] [INSPIRE].

[43] T. Bringmann, M. Doro and M. Fornasa, *Dark Matter signals from Draco and Willman 1: Prospects for MAGIC II and CTA*, *JCAP* **01** (2009) 016 [arXiv:0809.2269] [INSPIRE].

[44] A. Ibarra, M. Totzauer and S. Wild, *Higher order dark matter annihilations in the Sun and implications for IceCube*, *JCAP* **04** (2014) 012 [arXiv:1402.4375] [INSPIRE].

[45] M. Garny, A. Ibarra and S. Vogl, *Antiproton constraints on dark matter annihilations from internal electroweak bremsstrahlung*, *JCAP* **07** (2011) 028 [arXiv:1105.5367] [INSPIRE].

JHEP10(2014)183